# Chemical hypoxia induces pro-inflammatory signals in fat-laden hepatocytes and contributes to cellular crosstalk with Kupffer cells through extracellular vesicles

Hernandez, Alejandra; Geng, Yana; Sepulveda, Rolando; Solis, Nancy; Torres, Javiera; Arab, Juan Pablo; Barrera, Francisco; Cabrera, Daniel; Moshage, Han; Arrese, Marco

*Published in:*
Biochimica et biophysica acta-Molecular basis of disease

*DOI:*
10.1016/j.bbadis.2020.165753



*Publication date:*
2020

Journal Pre-proof

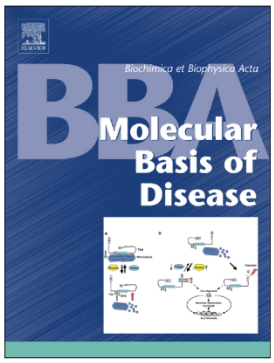


# Chemical hypoxia induces pro-inflammatory signals in fat-laden hepatocytes and contributes to cellular crosstalk with Kupffer cells through extracellular vesicles

Alejandra Hernandez, Yana Geng, Rolando Sepulveda, Nancy Solis, Javiera Torres, Juan Pablo Arab, Francisco Barrera, Daniel Cabrera, Han Moshage, Marco Arrese

PII: S0925-4439(20)30098-3

DOI: https://doi.org/10.1016/j.bbadis.2020.165753

Reference: BBADIS 165753

To appear in: *BBA - Molecular Basis of Disease*

Received date: 4 November 2019

Revised date: 6 February 2020

Accepted date: 27 February 2020

Please cite this article as: A. Hernandez, Y. Geng, R. Sepulveda, et al., Chemical hypoxia induces pro-inflammatory signals in fat-laden hepatocytes and contributes to cellular crosstalk with Kupffer cells through extracellular vesicles, *BBA - Molecular Basis of Disease*(2020), https://doi.org/10.1016/j.bbadis.2020.165753

# Chemical Hypoxia induces pro-inflammatory signals in fat-laden hepatocytes and contributes to cellular crosstalk with Kupffer cells through extracellular vesicles

Alejandra Hernandez[1,2], Yana Geng[2], Rolando Sepulveda[1], Nancy Solis[1], Javiera Torres[2], Juan Pablo Arab[1], Francisco Barrera[1], Daniel Cabrera[1], Han Moshage[3] and Marco Arrese[1,3 *]

[1]Departamentos de Gastroenterología y [2]Patología, Escuela de Medicina, Pontificia Universidad Católica de Chile. Santiago, Chile, [2]Department of Gastroenterology and Hepatology, University of Groningen, University Medical Center Groningen, Groningen, the Netherlands, [3]Centro de Envejecimiento y Regeneración (CARE), Departamento de Biología Celular y Molecular, Facultad de Ciencias Biológicas Pontificia Universidad Católica de Chile, Santiago, Chile

**Keywords**: Nonalcoholic fatty liver disease; fatty liver disease; hepatology; hypoxia, liver injury, steatosis, apoptosis.

**Running title:** *Hypoxia and experimental NAFLD*

**Abstract word count:** 257
**Word count:** (excluding references) 4660
**Tables:** 0, **Figures:** 12

***Address for correspondence:**

Marco Arrese, MD
Pontificia Universidad Católica de Chile,
Departamento de Gastroenterología
Facultad de Medicina
Marcoleta 367
8330024
Santiago, CHILE , e-mail: marrese@med.puc.cl

**ABSTRACT**

**Background**. Obstructive sleep apnea syndrome (OSAS) is associated to intermittent hypoxia (IH) and is an aggravating factor of non-alcoholic fatty liver disease (NAFLD). We investigated the effects of hypoxia in both *in vitro* and *in vivo* models of NAFLD.

**Methods**: Primary rat hepatocytes treated with free fatty acids (FFA) were subjected to chemically induced hypoxia (CH) using the hypoxia-inducible factor-1 alpha (HIF-1α) stabilizer cobalt chloride (CoCl2). Triglyceride (TG) content, mitochondrial superoxide production, cell death rates, cytokine and inflammasome components gene expression and protein levels of cleaved caspase-1 were assessed. Also, Kupffer cells (KC) were treated with conditioned medium (CM) and extracellular vehicles (EVs) from hypoxic fat-laden hepatic cells. The choline deficient L-amino acid defined (CDAA)-feeding model used to assess the effects of IH on experimental NAFLD *in vivo*.

**Results**: Hypoxia induced HIF-1α in cells and animals. Hepatocytes exposed to FFA and CoCl2 exhibited increased TG content and higher cell death rates as well as increased mitochondrial superoxide production and mRNA levels of pro-inflammatory cytokines and of inflammasome-components interleukin-1β, NLRP3 and ASC. Protein levels of cleaved caspase-1 increased in CH-exposed hepatocytes. CM and EVs from hypoxic fat-laden hepatic cells evoked a pro-inflammatory phenotype in KC. Livers from CDAA-fed mice exposed to IH exhibited increased mRNA levels of pro-inflammatory and inflammasome genes and increased levels of cleaved caspase-1.

**Conclusion:** Hypoxia promotes inflammatory signals including inflammasome/caspase-1 activation in fat-laden hepatocytes and contributes to

cellular crosstalk with KC by release of EVs. These mechanisms may underlie the aggravating effect of OSAS on NAFLD. [Abstract word count: 257]

**Abbreviations used in this paper**:

OSAS: obstructive sleep apnea syndrome

IH: intermittent hypoxia

NAFLD: non-alcoholic fatty liver disease

NAFL: non-alcoholic fatty liver

NASH: non-alcoholic steatohepatitis

NLRP3: NOD-like receptor Pyrin Domain Containing 3

GSDMD: gasdermin D

KC: Kupffer cells

TG : triglyceride

IL: interleukin

TNF-α: tumor necrosis factor-alpha

HIF-1α: hypoxia inducible factor 1 alpha

EVs: extracellular vesicles

FBS: fetal bovine serum

FFA: free fatty acids

CM: conditioned medium

AUF: Arbitrary units of fluorescence

PBS: phosphate-buffered saline

LDH: Lactate dehydrogenase

NTA: nanoparticle tracking analysis

ASC: Apoptosis-Associated Speck-Like Protein Containing CARD

## 1.- INTRODUCTION

In recent years, obstructive sleep apnea syndrome (OSAS), a common sleep disorder characterized by recurrent closure of the upper airways during sleep, has been suggested to modulate the severity of different metabolic disorders (1, 2). The hallmark of OSAS is the occurrence of intermittent hypoxia (IH) leading to tissue hypoxia and promoting oxidative stress, inflammation and a myriad of multi-organ pathophysiological effects (3). Among conditions in which OSAS acts as both a potential inducer and as an aggravating factor is non-alcoholic fatty liver disease (NAFLD), the commonest liver disease worldwide (4-6). NAFLD describes a clinicopathological entity defined by the presence of a spectrum of hepatic histological changes ranging in severity from isolated steatosis (also termed non-alcoholic fatty liver [NAFL]) to steatohepatitis (named non-alcoholic steatohepatitis, NASH) through to advanced fibrosis and cirrhosis (7, 8). Development of steatosis is closely linked to both overweight and obesity as well as to insulin resistance and transition from isolated steatosis to more advanced stages of the disease occurs only in a minority of NAFLD patients. Multiple factors influence NAFLD development and progression including individual's genetic background, environmental factors and the presence of a myriad of comorbidities including OSAS (6, 9).

The main mechanisms of hepatocellular damage in NAFLD include those related to lipotoxicity, mitochondrial dysfunction, formation of reactive oxygen species, endoplasmic reticulum stress and disturbed autophagy ultimately leading to hepatocyte injury and death that triggers hepatic inflammation, hepatic stellate cell activation, and progressive fibrogenesis, thus driving disease progression (8, 10-12).

In addition, recent studies have shown that inflammasome activation is also one of the key events in NAFLD progression (13-15). Specifically, the NOD-like receptor Pyrin Domain Containing 3 (NLRP3) inflammasome has been recognized to be involved in the progression of liver damage in experimental *in vitro* (hepatocytes and immune liver cells) and *in vivo* models of NASH (16-18) and also in human studies (19). NLRP3 inflammasome mediates the maturation of inactive pro-caspase-1 into active cleaved caspase-1, which cleaves gasdermin D (GSDMD) that in turn determine the activation of the pro-inflammatory cytokines interleukin [IL]-1β and IL-18, which amplify the pathological phenomena in NAFLD by promoting inflammation and pyroptotic cell death (20). Of note, the progression of damage in NAFLD also involves the participation of other liver-resident cells such as macrophages or Kupffer cells (KC) as well as the recruitment of inflammatory cells from the periphery (21-23).

With regard to the pathophysiological connections between OSAS and NAFLD, existing data indicate that OSAS may relate to both NAFLD occurrence as well as disease progression. Of note, several studies have shown that IH is able to induce metabolic alterations such as insulin resistance and increased liver triglyceride (TG) accumulation as well as increased oxidative stress and increased inflammation, which are related to steatosis development and hepatocellular damage, respectively (24-26). Hepatic TG accumulation in the setting of OSAS may result from hypoxia-related changes in lipid metabolic pathways such as a decrease in fatty acid β-oxidation and increased *de novo* lipogenesis (5, 27). Also, IH has been shown to promote pro-inflammatory effects in animal models of NAFLD modulating inflammatory cytokine production (i.e. tumor necrosis factor-alpha [TNF-α] and IL-6) (28, 29). Although

some studies suggest a relevant role of hypoxia, likely through induction of the hypoxia inducible factor 1 alpha (HIF-1α), in promoting hepatocellular cell death and the generation of pro-inflammatory signals in several experimental settings (30), assessment of these phenomena in the context of NAFLD has been less explored (5, 31).

In the present study, we aimed to assess the effects of hypoxia on cellular lipid accumulation, hepatocellular death and pro-inflammatory signals including those related to the NLRP3 inflammasome leading to caspase-1 activation in *in vitro* and *in vivo* models of NAFLD. Moreover, we explored whether hypoxia modulates cellular crosstalk between hepatocytes and resident macrophages (i.e. KCs) in the setting of NAFLD and if this crosstalk involves the release of extracellular vesicles (EVs) from hepatocytes. Of note, EVs have been recently recognized as playing an important role in amplifying the inflammatory response in NASH (32, 33) but few data exist on the potential role of hypoxia in modulating their release. We found that hypoxia induces hepatocellular damage in fat-laden hepatocytes that involves NLRP3 inflammasome-associated caspase-1 activation and increased mitochondrial superoxide production leading to increased cell death rates by multiple mechanisms including apoptosis and pyroptosis. Also, hypoxia contributes to evoking a pro-inflammatory response in Kupffer cells by a mechanism that involves EVs release from fat-laden hepatocytes. These observations partially clarify the mechanisms underlying the aggravating effect of OSAS on NAFLD.

## 2.- MATERIALS AND METHODS

### *2.1 Animals*

Specified pathogen-free male Wistar rats (220–250 g; Charles River Laboratories Inc., Wilmington, MA, USA) and male C57bl6 mice [purchased from Jackson Laboratories (Bar Harbor, ME, USA)] were used in the present study. Animals were housed under standard laboratory conditions with free access to standard laboratory chow diet and water. All experiments were carried out according to the Dutch and Chilean laws on the welfare of laboratory animals and guidelines of the local institutional animal care and use committees of the Pontificia Universidad Católica de Chile and ethics committee of University of Groningen for care and use of laboratory animals. All efforts were made to minimize animals suffering and to reduce the number of animals used.

### *2.2 Cell isolation techniques, culture conditions, cell surface markers detection and use of liver-derived cell lines*

To conduct the experiments described below we used both primary rat hepatocytes and KC. Isolation techniques used are described elsewhere (34, 35) and in the Supplementary material file. Details of culture conditions and KC cell surface markers detection are also provided in that section. The human hepatocellular carcinoma cell line HepG2 (American Type Culture Collection [ATCC] HB-8065, Manassas, VA, USA) was used to carry out experiments involving EVs isolation after treatment with FFA. Culture conditions are described in the supplementary material file.

### *2.3 Treatment with free fatty acids and chemical hypoxia induction*

In order to assess the effects of hypoxia in fat-laden liver cells, hepatocytes were incubated with a mixture of free fatty acids (FFA) consisting of oleic acid (500 µmol/L) and palmitic acid (250 µmol/L) in an aqueous solution of BSA as described (36). Incubations were carried out with or without Cobalt(II) chloride (CoCl2; Sigma Aldrich, Saint Louis, MO, USA) (200 µmol/L) for 24 hours to induce chemical hypoxia (37). CoCl2 is a well-known hypoxia-mimetic agent, that mimics hypoxia/ischemic conditions by stabilization of hypoxia-inducible factor HIF-1α (38). Control cells were treated with BSA alone. To obtain the corresponding conditioned medium (CM), after treatment, hepatocyte culture medium was replaced by FBS-free medium for an additional 24 hours. CM from different treatments were added to KC for 24 hours in order to explore the possibility that hypoxia modulates hepatocytes-KC cellular crosstalk.

***2.4 Oil red O cell staining and TG measurement***

Primary rat hepatocytes cultured on glass cover slides were treated with FFA and CoCl2 for 24 h. Hepatocytes were then washed with phosphate-buffered saline (PBS) twice, and then fixed with 4% formalin for 10 minutes. Cells were washed with 60% isopropanol twice and stained with oil-red-O solution for 10 minutes at room temperature. Then, cells were washed with 60% isopropanol and washed in distilled water for 5 minutes. Then cells were incubated with hematoxylin/eosin solution for 1 minute and washed with distilled water for 5 minutes. Slices were mounted using 1 drop of glycerin-gelatin solution. Stained lipid droplets in cells were examined using a slide scanner, Nanozoomer™ (Hamamatsu Photonics K.K., Shizuoka, Japan). Intracellular TG content was determined using TG Quantification Assay kit (ab65336,

Abcam, Cambridge, UK) according to the manufacturer's instructions and normalized to protein concentration.

***2.5 Apoptosis measurement***

Caspase-3 fluorometric assay was used to determine apoptosis induced by FFA and/or CoCl2 in freshly isolated mouse hepatocytes. After treatment, hepatocytes were scraped and cell lysates were obtained by three cycles of freezing (−196°C) in liquid nitrogen and thawing (37°C) followed by centrifugation for 5 minutes at 13,000g. Caspase-3 enzyme activity was assayed as described previously (39). Arbitrary units of fluorescence (AUF) were quantified in a spectrofluorometer at an excitation wavelength of 380 nm and an emission wavelength of 430 nm.

***2.6 Assessment of cell death associated to disrupted cellular membrane integrity***

SYTOX™ Green nucleic acid stain (Invitrogen, S7020, Carlsbad, CA, USA) was used to determine cell death induced by FFA and/or CoCl2 in hepatocytes (40). Cells were cultured in 12-well plates. After treatment, diluted SYTOX Green solution (1:40.000/HBSS) was added to the plates for at least 15 minutes at 37°C, 5% CO2. SYTOX™ Green enters the cell upon loss of membrane integrity and binds to DNA acting as a counterstain that can be analyzed when excited at 488 nm. A Leica fluorescence microscope was used at that wavelength of for detection of necrotic cells, which were quantified using Image J software. Lactate dehydrogenase (LDH) release was assessed as described in the Supplementary materials file. Additionally, we assessed the caspase-cleaved gasdermin-N domain (GSDMD-N) to confirm pyroptotic cell death by Western blot to evaluate the occurrence of pyroptotic cell death (19).

### *2.7 Mitochondrial superoxide detection*

At the end of 24h-long incubations, hepatocytes were washed once with warm HBSS followed by incubation with 200 nmol/L MitoSOX™ Red Molecular Probes (Invitrogen™, Carlsbad, CA,USA) in William's E medium for 15 min at 37°C protected from light in order to detect mitochondrial superoxide production (41). Then, cells were washed with warm HBSS and mounted onto glass slides using DAPI staining solution (Invitrogen™, Carlsbad, CA,USA). The fluorescence analyses were immediately recorded using a fluorescent microscope at a wavelength of 510/580 nm (Ex/Em) by a Leica microscope (Leica Microsystems GmbH, Wetzlar, Germany). Quantification of fluorescence in microscopic images of MitoSOX was performed using Image J software.

### *2.8 Western Blot analyses and antibodies*

Protein levels expression were detected by total cell lysate subjected to western blot as previous described (42). The following antibodies were used: Monoclonal mouse anti-HIF1α 1:1000 (Abcam, USA); monoclonal mouse anti-GSDMDC1 1:500 (Santa Cruz Biotechnology, Dallas, TX, USA); polyclonal rabbit anti-CASP-3 (Cell Signaling Technology, Leiden, The Netherlands); monoclonal mouse anti-CASP1 1:500 (Santa Cruz Biotechnology, Dallas, TX, USA); monoclonal mouse anti-CD81 1:1000 (Invitrogen™, Carlsbad, CA,USA) and monoclonal rabbit anti-Bcl-2 1:1000 (Abcam, UK) were used in combination with appropriate peroxidase-conjugated secondary antibodies. Monoclonal mouse anti-tubulin or actin were used as loading controls (Sigma, Life Sciences, Merck KGaA, Darmstadt, German). Blots were analyzed in a

ChemiDoc XRS system (Bio-Rad, Hercules, CA, USA). Protein band intensities were quantified by ImageLab software (BioRad, Hercules, CA, USA).

### *2.9 RNA isolation and quantitative real-time reverse transcription polymerase chain reaction (qRT-PCR)*

Total RNA was isolated with TRI-reagent (Sigma-Aldrich, Saint Louis, MO, USA) according to the manufacturer's instructions. Quantification of RNA was measured with the Nanodrop spectrophotometer (Thermo Scientific, Wilmington, DE, USA). Reverse transcription (RT) was performed using 2.5 μg of total RNA. Quantitative Real Time PCR (qRT-PCR) was carried out in a StepOnePlus™ (96-well) PCR System (Applied Biosystems, Thermofisher, Waltham, MA, USA) using TaqMan method or SYBR Green method. The sequences of the probes and primer sets are described in the Supplementary materials file. mRNA levels were normalized to the housekeeping gene 18S and further normalized to the mean expression level of the control group. Relative gene expression was calculated via the $2^{-ddCT}$.

### *2.10 Enzyme-linked immunosorbent assay (ELISA) of Interleukin-1beta*

Levels of pro-inflammatory cytokine of IL-1β in primary rat KC were assessed by the ELISA kit (ab100768, Abcam, Cambridge, UK), according to the manufacturer's instructions.

### *2.11 EVs isolation and characterization*

EVs were collected from culture media of HepG2 cells as described previously (43) and summarized in the Supplementary materials file. Nanoparticle tracking analysis (NTA) was performed using NanoSight NS300 instrumentation (Marvel, Egham, UK) that uses both light scattering and Brownian motion analysis for nanoparticle

characterization. We further caharacterized EVs using Transmission electron microscopy. Sample preparation and details of these analysis are described in the Supplementary materials file.

### *2.12 Treatment of KC cells with and extracellular vesicles*

Rat primary KC were incubated with FBS-free William's E medium and exposed to 15 µg of EVs that were isolated from HepG2 cells treated with CoCl2 + FFA for 24h. After 24h of EVs treatment, KC were harvested to continue with analyses by quantitative PCR.

### *2.13 Effects of intermittent hypoxia in experimental NASH*

Animal experiments were approved by the institutional animal care and use committee (Comité de ética y bienestar Animal, Escuela de Medicina, Pontificia Universidad Católica de Chile, CEBA 100623003). Male C57BL/6 mice aged 10 weeks at the beginning of the study and divided into four experimental groups (n = 4–8) receiving either choline-deficient amino acid-defined (CDAA) diet (Catalog # 518753, Dyets Inc. Bethlehem, PA) to induce NASH or the choline-supplemented L-amino acid defined (CSAA, Catalog # 518754, Dyets Inc. Bethlehem, PA) diet as control for 22 weeks as previously described (16, 44). Animals were exposed to IH or normoxia (chambers 41x22x35 cm, COY lab products™, Grass Lake, MI, USA) during the last 12 weeks of the experimental or control feeding period. IH regimen consisted in 30 events/hour of hypoxic exposures for 8 hour/day during the rest cycle, between 9 am and 5 pm. This cycle was repeated 7 days a week for 12 consecutive weeks. After ending the study, mice were anesthetized (ketamine 60 mg/kg plus xylazine 10 mg/kg intraperitoneally) and then euthanized by exsanguination. Serum and liver tissue

samples were collected and processed or stored at −80 °C until analyzed. Gene expression and protein analyses were carried out as described above. Positive control of hypoxia induction was evaluated by measurement of hepatic gene expression of HIF-1α.

### *2.14 Histological Studies*

Liver steatosis was analyzed on paraformaldehyde-fixed liver sections stained with Oil Red-O staining that show lipid deposits in red color on frozen 7 µm liver cryosections. A blinded pathologist (J.T.) assigned a score for steatosis, inflammation and fibrosis as described (44). Scores were given as it follows: Steatosis: grade 0, none present; grade 1, steatosis of ≤25% of parenchyma; grade 2, steatosis of 26–50% of parenchyma; grade 3, steatosis of 51–75% of parenchyma; grade 4, steatosis of ≥76% of parenchyma and inflammation: grade 0, no inflammatory foci; grade 1, 1–5 inflammatory foci per high power field; grade 2, >5 inflammatory foci/high power field. Fibrosis was estimated qualitatively in Sirius red-stained samples.

### *2.15 Hepatic triglyceride determination*

Hepatic triglyceride content (HTC) was using 40-50 mg of homogenized liver tissue in 1.5 ml of a $CHCl_3$-$CH_3OH$ mixture (2:1, v/v), followed by a Folch extraction described previously (16, 31).

### *2.16 Statistical Analyses*

Analyses were performed using GraphPad software (version 5.03, GraphPad Software Inc., CA, USA). Statistical analyses were performed using one-way analysis of variance (ANOVA) with a post-hoc Bonferroni correction with multiple-comparison test or by parametric t-tests when needed. All the results are presented as a mean of at least 3

independent experiments ± SEM. Values were represented as absolute number, normalized data respect to control or percentage for categorical variables. Regarding in vitro assays, independent experiments means different cell plates harvested from at least three animals. Regarding in vivo assays, independent experiments means at least three different animal samples. All the results were analyzed and plotted using GraphPad software (version 5.03, GraphPad Software Inc., CA, USA). Statistics with a value of $p<0.05$ were considered significant.

## 3.- RESULTS

**3.1 Hypoxia induces HIF-1α and promotes the increase of lipid droplets in fat-laden hepatocytes:** To investigate whether hypoxia exacerbates lipotoxicity in an *in vitro* model of experimental NASH, we treated fat-laden primary rat hepatocytes with CoCl2, a hypoxia mimetic agent that promotes the accumulation of HIF-1α (45, 46). As expected, chemical hypoxia increased protein levels of HIF-1α in both control and fat-laden hepatocytes as determined by Western Blot technique (Figure 1). Interestingly, we also observed an increase in the number of intracellular lipid droplets, determined by Oil Red O staining (Figure 2a) and of hepatocyte TG content (Figure 2b) after treatment with a mixture of FFA, which was higher in cells concomitantly treated with CoCl2 indicating that the hypoxic condition promotes an increase intracellular lipid deposition in this model.

**3.2 Hypoxia increases apoptotic and pyroptotic cell death in fat-laden hepatocytes:** To evaluate whether the induction of chemical hypoxia exacerbates lipotoxic cell damage and death, we determined protein levels and activity of caspase-3 to assess apoptotic cell death and used SYTOX™ Green nucleic acid stain and LDH leakage to evaluate cell death associated to disrupted cellular membrane integrity. Additionally, we assessed the caspase-cleaved gasdermin-N domain (GSDMD-N) to evaluate pyroptotic cell death (19). While CoCl2 did not influence cleaved caspase-3 and caspase 3 activity in normal hepatocytes, steatotic hepatocytes undergoing chemical hypoxia displayed a two-fold increase in cleaved caspase-3 (Figure 3a) and six-fold increase in caspase-3 activity (Figure 3b) compared to control cells. Of note, treatment with a mixture of FFA alone led to a two-fold increase (n.s.) in caspase 3

activity suggesting that chemical hypoxia exacerbates lipotoxicity and apoptotic cell death in fat-laden hepatocytes. Also, using SYTOX™ Green nucleic acid stain (Figure 4a) and measurement of cellular LDH leakage (Figure 4b), we found that chemical hypoxia also increased cell death rate associated to losing plasma membrane integrity of fat-laden hepatocytes compared to control cells or cells treated only with FFA. Furthermore, protein levels of GSDMD-N, which is considered a pyroptosis executor (19), increased three-fold in hypoxic fat-laden hepatocytes compared to control cells (Figure 4c).

**3.3 Hypoxia increases superoxide production by mitochondria in steatosis *in vitro:*** Recent studies on the pathogenesis of NASH have described an important role for mitochondrial oxidative stress (47-50). To evaluate this issue, we examined the levels of mitochondrial superoxide generation in fat-laden hepatocytes treated with CoCl2. Fat-laden hepatocytes undergoing hypoxia exhibited ten-fold higher levels of mitochondrial superoxide fluorescence determined by MitoSOX™ compared to control cells. CoCl2 or FFA treatment alone did not determine significant changes in MitoSOX™ fluorescence intensity (Figure 5). These data indicate that chemical hypoxia in fat-laden hepatocytes promotes oxidative stress by an increase of mitochondrial superoxide production.

**3.4 Effect of CoCl2-induced chemical hypoxia on the expression of pro-inflammatory cytokines and inflammasome components in fat-laden hepatocytes**: To evaluate whether chemical hypoxia promotes an inflammatory phenotype in fat-laden hepatocytes, we measured mRNA levels of the pro-inflammatory cytokines TNF-a, IL-6 as well as of NLRP3 inflammasome components in

cultured cells treated or not with FFA and CoCl2. As shown in figure 6, steatotic hepatocytes treated with CoCl2 displayed a marked increase in mRNA levels of IL-1β (2.5-fold), TNF-α (2-fold), and of IL-6 (9-fold) compared to non-treated cells. Also, mRNA levels of NLRP3 and Apoptosis-Associated Speck-Like Protein Containing CARD (ASC) were also significantly increased in fat-laden hepatocytes undergoing hypoxia compared with cells treated solely with FFA (Figure 6).

**3.5 CoCl2-treatment of fat-laden hepatocytes increases protein expression of caspase-1:** The inflammasome is a multiprotein complex needed for caspase-1 processing and the subsequent activation of the inflammatory cytokines IL-1β and IL-18, which has been involved in the pathogenesis of NAFLD/NASH (20). Therefore, we examined the protein expression of caspase-1 in both freshly isolated control hepatocytes and hepatocytes treated with FFA as described above treated or not with CoCl2 in order to explore the effects of chemical hypoxia on inflammasome activation. While FFA treatment did not influence protein expression of caspase-1, CoCl2 treatment increased the protein levels of pro-caspase-1 (inactive form) and cleaved caspase-1 (p20 and p10 active forms) in hepatocytes irrespective if they were fat-laden or not (Figure 7) These data suggest that chemical hypoxia is able to activate the inflammasome complex in hepatocytes resulting in caspase-1 activation.

**3.6 Conditioned medium of steatotic hepatocytes subjected to hypoxia increases pro-inflammatory cytokines in Kupffer cells:** To explore whether hypoxic, fat-laden hepatocytes can trigger pro-inflammatory responses in KC, we performed experiments exploring the effects of exposing KCs to CM obtained from fat-laden hepatocytes undergoing chemical hypoxia. We first profiled isolated KC assessing the

expression of two typical macrophage markers [CD-68 as macrophage marker and CD-163 as KC marker (51)] by immunofluorescence (Figure 8) confirming the quality of KC isolation. Then, we observed that CM from steatotic hepatocytes subjected to hypoxia increases KC's mRNA levels of pro-inflammatory genes and decreased mRNA levels of the anti-inflammatory cytokine IL-10, without affecting gene expression of the classic KC M2 marker gene arginase-1 (Arg-1) (Figure 9a). Furthermore, protein levels of IL-1β were significantly higher in KC treated with CM from fat-laden hepatocytes undergoing chemical hypoxia compared with all other groups (Figure 9b). Treatment of cultured rat KC with CM obtained from hepatocytes treated with FFA alone also resulted in higher protein levels of IL-1β in KC compared to control cells (Figure 9b) but this effect was less intense than that observed with CM from steatotic hepatocytes undergoing chemical hypoxia, suggesting that hypoxia exacerbates the expression of this pro-inflammatory cytokine. These data support the hypothesis that hypoxic and steatotic hepatocytes release signals that promote a pro-inflammatory phenotype in KC.

**3.7. Extracellular vesicles increased in CM from fat-laden hepatocellular cell line exposed to CoCl2 and promoted pro-inflammatory genes expression in KC:** To explore if EVs released from fat-laden hepatocytes undergoing hypoxia play a role in promoting a pro-inflammatory effects in KC, EVs were collected from culture media obtained from cultured HepG2 cells. We first explored if CM from HepG2 cells exposed to the different treatments evoked proinflammatory signals in KC. Results of these experiments are shown in Supplementary figure 2. As shown in this figure, similar to the effects observed in experiments involving hepatocytes, CM did determine

increased expression of proinflammatory genes in KC, a decrease in the expression of IL-10 and had no effect on Arginase-1 expression. We then explored the effects of HepG2-derived EVs on KC and compared the observed effects with the effect of treatment with the EVs-free fraction. We first characterized EVs by transmission electron microscopy as well as by Western blot detection of the presence of the EVs marker CD81 and the absence of the mitochondrial protein Bcl-2 in all EV fractions (Figure 10a and Supplementary Figure 1). Of note, the size and concentration of HepG2-derived EVs were determined by NTA. Interestingly, we found an increase of EVs in culture media from fat-laden cells exposed to CoCl2 ($6.0 \times 10^{11}$ particles/mL) compared to culture media from control cells ($9.5 \times 10^{10}$ particles/mL) (Figure 10b). As shown in this figure, the average size of EVs obtained from culture media of control cells was 150 nm while those EVs obtained from fat-laden HEPG2 cells undergoing CoCl2 was 130 nm (n.s.). Next, we examined the response of KCs to treatment with HepG2-derived EVs. EVs from steatotic HepG2 cells treated with CoCl2 determined a marked increase in mRNA levels in KC of the following proinflammatory genes: IL-1β (2.0-fold), TNF-α (2.5-fold), iNOS (1.6-fold) and of IL-6 (2.2-fold) in comparison to treatment with EVs from non-treated cells, without affecting significantly gene expression of IL-10 and Arg-1 (Figure 10c). However, EV-free CM, as negative control to evaluate the specific effect of EVs, promoted an increased on iNOS gene expression in KC (1.4-fold), demonstrating that CM EV-free may contains soluble substances that induce the expression of this specific pro-inflammatory cytokine. Of note, treatment of KC with EVs obtained from HepG2 cells treated with FFA or CoCl2 alone did not evoke

significant changes in KC expression of pro-inflammatory genes (Supplementary Figure 3).

**3.8. Intermittent hypoxia in an experimental model of diet-induced non-alcoholic steatohepatitis increases the inflammatory phenotype:** To validate our *in vitro* findings, we investigated the effect of IH for 12 weeks in an animal model, the CDAA diet-induced NASH (16). To evaluate steatosis, liver sections were stained with Oil red O staining (Figure 11a) (Abcam, Cambridge, UK). Steatosis, inflammation and fibrosis was graded blindly by an experienced pathologist (J.T.) according to the NAS score. Specifically, the amount of steatosis (percentage of hepatocytes containing fat droplets) was scored as 0 (<5%), 1 (5–33%), 2 (>33–66%) and 3 (>66%). Although pathological scoring suggested a higher degree of steatosis in animals on CDAA diet and exposed to hypoxia compared to control animals and compared to animals on CDAA diet and normoxic conditions (Figure 11b), we did not observed significant differences in the hepatic TG levels between the CDAA-fed mice groups (Figure 11c). Also, no differences were found in NAS score when comparing CDAA-fed groups. However, mRNA levels of pro-inflammatory genes and NLRP3 inflammasome components significantly increased in animals with hypoxia on CDAA diet compared to all other groups (Figure 12). Finally, we tested the caspase-1 protein levels, which significantly increases in animals with hypoxia on CDAA diet (Figure 13). With these results, we verified that hypoxia promotes an aggravated the inflammatory phenotype in NASH and specifically influences inflammasome activation.

## 4.- DISCUSSION

NAFLD represents a highly frequent cause of liver disease, which is closely associated with obesity and insulin resistance (7, 52). Clinical observations suggest that patients with OSAS have a greater predisposition to develop NAFLD and NASH, the aggressive form of NAFLD, which is characterized by the presence of necro-inflammatory and fibrotic phenomena in the liver (5). Several studies have shown that OSAS, mainly through the occurrence of IH, can modulate hepatocellular damage by triggering proinflammatory and profibrotic signals (25, 26), but pathways underlying this effects are ill-defined. The present study used cellular models of NAFLD/NASH to explore potential synergistic interactions between hypoxia and FFA exposure. To that end, the hypoxia mimetic agent CoCl2 was used to treat fat-laden hepatocytes. Our findings suggest that indeed hypoxia determines a further increase in cellular TG content in FFA treated hepatocytes as well as increased mRNA levels of pro-inflammatory cytokines as well as those of the NLRP3 inflammasome components. These phenomena were also associated with increased mitochondrial superoxide levels and increased rates of cell death due to apoptosis and disruption of cell membrane, likely pyroptosis as suggested by the increase in GSDMD levels. Moreover, conditioned medium obtained from hypoxic fat-laden hepatocytes promoted an inflammatory phenotype in KC, which is known to be decisive for the amplification of the pathological phenomenon of NASH (12, 23). Additionally, in order to determine if the observed effects on KC could be mediated by EVs release from hepatocytes, we conducted further experiments in the human hepatoma cell line HepG2. We choose this approach for practical reasons since using this cell line the EVs isolation efficiency

is high. Our results showed that treatment of HepG2 with FFA and CoCl2 determines an increase in the release of EVs to the medium and that these EVs also evoke a pro-inflammatory response in rat KC in line with previous observations showing that released EVs from fat-laden hepatocytes can act in in macrophages and contribute to pro-inflammatory response in a paracrine fashion (15).

Finally, we found correlates of our *in vitro* NASH model findings in an animal model of NASH induced by feeding a CDAA diet. In the latter experiments, we also confirmed that IH promotes NLRP3 inflammasome activation in the setting of NASH. Collectively taken, these findings indicate that hypoxia may influence NAFLD development and progression by acting at different levels including promotion of further lipid accumulation as well as enhancement of liver inflammation and hepatocellular death. Of note, recent rodent studies indicate that hypoxia may be also linked to liver fibrosis, a key prognostic feature of NASH (8). In fact, Mersarwi et al. demonstrated that HIF-1α deletion in hepatocytes protects against the development of liver fibrosis in a mouse model of NAFLD (53). This observation adds to our data and support the concept that hypoxia contributes to NAFLD progression influencing critical steps of the disease.

Experimental data on the effects of hypoxia in NAFLD models is scarce and mainly restricted to whole animal studies (53, 54). No data is available on the effects of hypoxia in cellular models of NAFLD/NASH (36). To assess this, we used the hypoxia mimetic compound CoCl2, which induces chemical hypoxia by stabilizing HIF-1α and 2α (38). This model is well accepted and has several advantages over alternatives such as the hypoxia chamber or a $CO_2$ incubator with regulated oxygen levels, which

are less available, most costly and provide a less stable experimental conditions (38). CoCl2 has been previously used in normal isolated hepatocytes (38, 45) but not in fat-laden cells underlying the novelty of our approach. Of note, previous studies as well as experiments of our laboratory on hepatocyte cell lines have demonstrated the non-toxic effect of CoCl2 at concentrations not exceeding 400 μmol/L for 24 hours as previously described (55). On the other hand, FFA treatment using combination of OA and PA effectively induced TG accumulation in the absence of lipoapoptosis (56). In spite of these advantages and, although CoCl2-induced chemical hypoxia is a suitable model to assess the effects of hypoxia in cellular models, we acknowledge that this model reproduces only some of the effects generated by a decrease in oxygen supply, which limit the generalizability of our results until they are confirmed in other models.

The observed hypoxia-related increases in intracellular lipid droplets and TG content in fat-laden hepatocytes is consistent with previous studies that indicate that hypoxia, through HIF-1α, promotes an increase in lipid biosynthesis causing TG accumulation (57, 58). We did not observe a marked increase in lipid content in cells treated solely with CoCl2, which may relate to length of treatment and experimental conditions. We also did not find an increase in the in vivo CDAA-feeding NASH model. We think that this may be related to the fact that this particular model determines severe steatosis and inflammation (59) and that therefore is difficult to observe subtle changes.

With regard to the effects of chemical hypoxia on cell death of FFA treated hepatocytes, qualitative determination of apoptosis, necrosis and pyroptosis using determination of caspase-3 cleavage, caspase-3 activity, SYTOX green staining, LDH

release and GSDMD-N were carried out as performed in previous studies (56, 60). While, treatment with CoCl2 or FFA alone did not induce a significant increase in apoptosis compared to control conditions, CoCl2 treatment of fat-laden hepatocytes did increase cleaved caspase-3 and caspase-3 activity reflecting ongoing apoptosis. The same observation was made regarding cell death associated to a disrupted plasma membrane, by SYTOX Green and LDH leakage measure, as an increased number of necrotic death cells was observed in steatotic hepatocytes subjected to hypoxia. Given the fact that hypoxia was associated to increase of GSDMD cleavage and up-regulation of inflammasome components, it is likely that pyroptosis also contributed to cell death of fat-laden hepatocytes undergoing chemical hypoxia. Of note, it has been suggested that pyroptosis may be an inflammatory link related to the progression from bland steatosis to NASH, as NLRP3 activation is not present in animal model of isolated steatosis without inflammation (61). Additionally, we observed a significant increase in mitochondrial superoxide levels in the fat-laden hepatocytes exposed to chemical hypoxia. Interestingly, increased mitochondrial superoxide generation has been correlated to mitochondrial dysfunction, oxidative damage, cellular death and pro-inflammatory effects in NASH (49, 62). Thus, this synergistic effect of hypoxia and FFA in hepatocytes with regard to mitochondrial superoxide generation, likely contributes to the observed increase in cell death when hepatocytes are exposed to both stimuli.

In addition to the observed effects on cell death and oxidative stress, chemical hypoxia also induced the expression of several inflammatory cytokines, including TNF-a, IL-6 and IL-1β, as well as of the components of the NLRP3 inflammasome (caspase-1, NLRP3 and ASC), in steatotic hepatocytes. The NLRP3 inflammasome activates pro-

caspase-1 into active caspase-1 (p10 and p20 cleaved caspase-1) that in turn cleaves pro-IL-1β into the mature form of IL-1β promoting amplification of liver inflammation and cell death (12). In recent years, caspase-1 has been studied extensively and has been shown to contribute to liver damage during the development of NASH (63, 64) and several studies have shown protective effects against liver damage when caspase-1 is inhibited (63). In our study, we evaluated the protein levels of caspase-1 (pro-caspase -1 and active cleaved-caspase-1) in hepatocytes. An increase in the total level of pro-caspase-1 was observed in hypoxic hepatocytes and hypoxic hepatocytes treated with FFA compared to the control conditions. Interestingly, cleaved-p-20 and p-10, the active isoforms of caspase-1, were only detected in hypoxic hepatocytes treated with FFA. These results are consistent with the observed up-regulation of inflammasome components and similar to those obtained by other authors in prostate epithelial cells undergoing hypoxia, showing increased NLRP3 inflammasome activation as determined by increased cellular levels of cleaved caspase-1 (65). Taken together, our results suggest that the induction of hypoxia in hepatocytes promotes susceptibility to damage by FFA, resulting in increased caspase-3 mediated apoptosis, (secondary) necrosis, pyroptosis and an inflammatory phenotype, characterized by increased expression of pro-inflammatory genes and protein levels of caspase-1.

Kupffer cells (KC) are involved in the pathogenesis of various liver diseases, including steatohepatitis (66). However, their role in the context of hepatocellular damage due to hypoxia remains poorly explored. KC are derived from circulating monocytes and, once established in the liver, fulfill multiple functions related to the immune system. KC maintain constant paracrine communication with neighboring hepatocytes,

stellate cells and endothelial cells through the signals that they receive from the extracellular environment (66). To verify the paracrine involvement of KC with steatotic hepatocytes in the context of hypoxia, KC were exposed to conditioned medium of hepatocytes subjected to different treatments. We documented that conditioned medium from steatotic and hypoxic hepatocytes induced a pro-inflammatory profile in KC. These novel results correlate well with recent studies showing micro-RNA-mediated cellular cross-talk between hepatocytes treated with ethanol and monocytes/ macrophages (67). As mentioned before, hepatocytes are able to modulate signaling pathways in macrophages, stellate cells and endothelial cells in a paracrine manner by cytokines, micro-RNAs and EVs (32). Our experiments involving isolation of EVs from HEPG2 cells strongly suggest that EVs participate in the cellular communication between steatotic and hypoxic hepatocytes and KC. This observations may have diagnostic and therapeutic implications (33).

In the present study, we also explored whether IH influences hepatic steatosis and the pro-inflammatory phenotype in an *in vivo* model of NASH. To this end, we assessed the effects of hypoxia for 22 weeks in CDAA-fed mice by evaluating liver histology and hepatic mRNA levels of pro-inflammatory cytokines. Our results showed a worsening of histological steatosis in CDAA-fed mice subjected to IH compared to those animals that did not undergo hypoxic conditions. However, we did not observe a corresponding increase in thepatic TG content. We think that this may be related to the fact that this particular model determines severe steatosis and inflammation (59) and that therefore is difficult to observe subtle changes.

With regard to inflammatory markers, CDAA-fed mice exposed to IH exhibited an increase of all inflammasome components (IL-1β, IL-18, NLRP3 and caspase-1) and other pro-inflammatory cytokines (IL-6, IFN-γ). Also, active caspase-1 level protein increased in livers from CDAA-fed mice exposed to IH, which correlates with the findings in the *in vitro* model. These observations support the concept that hypoxia may contribute to liver damage in the setting of NAFLD by activating the NLRP3 inflammasome. A recent study showing that IH activates the NLRP3 inflammasome in kidneys, which result in progressive renal injury (68) provides support to this notion. Although not explored in this study, this might have implications not only for hepatocellular injury but also for liver fibrosis development and hepatocarcinogenesis. (69, 70).

In summary, our results in *in vitro* and *in vivo* models of NAFLD/NASH support the notion that hypoxia plays an aggravating role in the setting of excessive lipid load in liver cells by influencing lipid deposition, hepatocellular death and pro-inflammatory signals, involving NLRP3 inflammasome activation. Moreover, our novel findings demonstrate that hypoxia modulates cellular crosstalk between steatotic hepatocytes and inflammatory cells (KCs). Future studies should focus on the characterization of the extracellular environment of hypoxic and steatotic hepatocytes to identify the hypoxia-specific factors and the mechanisms of hepatocellular damage at play in NASH.

**Funding:** This work was partially supported by the Chilean government through the Fondo Nacional de Desarrollo Científico y Tecnológico (FONDECYT 1150327 and 1119145 to M.A.) and the Comisión Nacional de Investigación Científica y Tecnológica (grant CONICYT PIA/Basal PFB12, Basal Centre for Excellence in Science and Technology to M.A.).

**5.- REFERENCES**

1. Drager LF, Lopes HF, Maki-Nunes C, Trombetta IC, Toschi-Dias E, Alves MJ, Fraga RF, et al. The impact of obstructive sleep apnea on metabolic and inflammatory markers in consecutive patients with metabolic syndrome. PLoS One 2010;5:e12065.

2. Gaines J, Vgontzas AN, Fernandez-Mendoza J, Bixler EO. Obstructive sleep apnea and the metabolic syndrome: The road to clinically-meaningful phenotyping, improved prognosis, and personalized treatment. Sleep Med Rev 2018;42:211-219.

3. Dempsey JA, Veasey SC, Morgan BJ, O'Donnell CP. Pathophysiology of sleep apnea. Physiol Rev 2010;90:47-112.

4. Agrawal S, Duseja A, Aggarwal A, Das A, Mehta M, Dhiman RK, Chawla Y. Obstructive sleep apnea is an important predictor of hepatic fibrosis in patients with nonalcoholic fatty liver disease in a tertiary care center. Hepatol Int 2015;9:283-291.

5. Mesarwi OA, Loomba R, Malhotra A. Obstructive Sleep Apnea, Hypoxia, and Nonalcoholic Fatty Liver Disease. Am J Respir Crit Care Med 2019;199:830-841.

6. Parikh MP, Gupta NM, McCullough AJ. Obstructive Sleep Apnea and the Liver. Clin Liver Dis 2019;23:363-382.

7. Rinella ME. Nonalcoholic fatty liver disease: a systematic review. JAMA 2015;313:2263-2273.

8. Arab JP, Arrese M, Trauner M. Recent Insights into the Pathogenesis of Nonalcoholic Fatty Liver Disease. Annu Rev Pathol 2018;13:321-350.

9. Chalasani N, Younossi Z, Lavine JE, Charlton M, Cusi K, Rinella M, Harrison SA, et al. The diagnosis and management of nonalcoholic fatty liver disease: Practice

guidance from the American Association for the Study of Liver Diseases. Hepatology 2018;67:328-357.

10. Noureddin M, Sanyal AJ. Pathogenesis of NASH: The Impact of Multiple Pathways. Curr Hepatol Rep 2018;17:350-360.

11. Ibrahim SH, Hirsova P, Gores GJ. Non-alcoholic steatohepatitis pathogenesis: sublethal hepatocyte injury as a driver of liver inflammation. Gut 2018;67:963-972.

12. Schuster S, Cabrera D, Arrese M, Feldstein AE. Triggering and resolution of inflammation in NASH. Nat Rev Gastroenterol Hepatol 2018;15:349-364.

13. Wree A, McGeough MD, Pena CA, Schlattjan M, Li H, Inzaugarat ME, Messer K, et al. NLRP3 inflammasome activation is required for fibrosis development in NAFLD. J Mol Med (Berl) 2014;92:1069-1082.

14. Wree A, Eguchi A, McGeough MD, Pena CA, Johnson CD, Canbay A, Hoffman HM, et al. NLRP3 inflammasome activation results in hepatocyte pyroptosis, liver inflammation, and fibrosis in mice. Hepatology 2014;59:898-910.

15. Cannito S, Morello E, Bocca C, Foglia B, Benetti E, Novo E, Chiazza F, et al. Microvesicles released from fat-laden cells promote activation of hepatocellular NLRP3 inflammasome: A pro-inflammatory link between lipotoxicity and non-alcoholic steatohepatitis. PLoS One 2017;12:e0172575.

16. Cabrera D, Wree A, Povero D, Solis N, Hernandez A, Pizarro M, Moshage H, et al. Andrographolide Ameliorates Inflammation and Fibrogenesis and Attenuates Inflammasome Activation in Experimental Non-Alcoholic Steatohepatitis. Sci Rep 2017;7:3491.

17. Csak T, Ganz M, Pespisa J, Kodys K, Dolganiuc A, Szabo G. Fatty acid and endotoxin activate inflammasomes in mouse hepatocytes that release danger signals to stimulate immune cells. Hepatology 2011;54:133-144.

18. Mridha AR, Wree A, Robertson AAB, Yeh MM, Johnson CD, Van Rooyen DM, Haczeyni F, et al. NLRP3 inflammasome blockade reduces liver inflammation and fibrosis in experimental NASH in mice. J Hepatol 2017;66:1037-1046.

19. Xu B, Jiang M, Chu Y, Wang W, Chen D, Li X, Zhang Z, et al. Gasdermin D plays a key role as a pyroptosis executor of non-alcoholic steatohepatitis in humans and mice. J Hepatol 2018;68:773-782.

20. Guo H, Callaway JB, Ting JP. Inflammasomes: mechanism of action, role in disease, and therapeutics. Nat Med 2015;21:677-687.

21. Cha JY, Kim DH, Chun KH. The role of hepatic macrophages in nonalcoholic fatty liver disease and nonalcoholic steatohepatitis. Lab Anim Res 2018;34:133-139.

22. Yu Y, Liu Y, An W, Song J, Zhang Y, Zhao X. STING-mediated inflammation in Kupffer cells contributes to progression of nonalcoholic steatohepatitis. J Clin Invest 2019;129:546-555.

23. Arrese M, Cabrera D, Kalergis AM, Feldstein AE. Innate Immunity and Inflammation in NAFLD/NASH. Dig Dis Sci 2016;61:1294-1303.

24. Drager LF, Li J, Reinke C, Bevans-Fonti S, Jun JC, Polotsky VY. Intermittent hypoxia exacerbates metabolic effects of diet-induced obesity. Obesity (Silver Spring) 2011;19:2167-2174.

25. Savransky V, Nanayakkara A, Vivero A, Li J, Bevans S, Smith PL, Torbenson MS, et al. Chronic intermittent hypoxia predisposes to liver injury. Hepatology 2007;45:1007-1013.

26. Savransky V, Reinke C, Jun J, Bevans-Fonti S, Nanayakkara A, Li J, Myers AC, et al. Chronic intermittent hypoxia and acetaminophen induce synergistic liver injury in mice. Exp Physiol 2009;94:228-239.

27. Liu Y, Ma Z, Zhao C, Wang Y, Wu G, Xiao J, McClain CJ, et al. HIF-1alpha and HIF-2alpha are critically involved in hypoxia-induced lipid accumulation in hepatocytes through reducing PGC-1alpha-mediated fatty acid beta-oxidation. Toxicol Lett 2014;226:117-123.

28. Briancon-Marjollet A, Monneret D, Henri M, Joyeux-Faure M, Totoson P, Cachot S, Faure P, et al. Intermittent hypoxia in obese Zucker rats: cardiometabolic and inflammatory effects. Exp Physiol 2016;101:1432-1442.

29. Kang HH, Kim IK, Lee HI, Joo H, Lim JU, Lee J, Lee SH, et al. Chronic intermittent hypoxia induces liver fibrosis in mice with diet-induced obesity via TLR4/MyD88/MAPK/NF-kB signaling pathways. Biochem Biophys Res Commun 2017;490:349-355.

30. Ju C, Colgan SP, Eltzschig HK. Hypoxia-inducible factors as molecular targets for liver diseases. J Mol Med (Berl) 2016;94:613-627.

31. van der Graaff D, Kwanten WJ, Francque SM. The potential role of vascular alterations and subsequent impaired liver blood flow and hepatic hypoxia in the pathophysiology of non-alcoholic steatohepatitis. Med Hypotheses 2019;122:188-197.

32. Eguchi A, Feldstein AE. Extracellular vesicles in non-alcoholic and alcoholic fatty liver diseases. Liver Res 2018;2:30-34.

33. Malhi H. Emerging role of extracellular vesicles in liver diseases. Am J Physiol Gastrointest Liver Physiol 2019;317:G739-G749.

34. Moshage H, Casini A, Lieber CS. Acetaldehyde selectively stimulates collagen production in cultured rat liver fat-storing cells but not in hepatocytes. Hepatology 1990;12:511-518.

35. Damba T, Zhang M, Buist-Homan M, van Goor H, Faber KN, Moshage H. Hydrogen sulfide stimulates activation of hepatic stellate cells through increased cellular bio-energetics. Nitric Oxide 2019;92:26-33.

36. Chavez-Tapia NC, Rosso N, Tiribelli C. In vitro models for the study of non-alcoholic fatty liver disease. Curr Med Chem 2011;18:1079-1084.

37. Pecoraro M, Pinto A, Popolo A. Inhibition of Connexin 43 translocation on mitochondria accelerates CoCl2-induced apoptotic response in a chemical model of hypoxia. Toxicol In Vitro 2018;47:120-128.

38. Munoz-Sanchez J, Chanez-Cardenas ME. The use of cobalt chloride as a chemical hypoxia model. J Appl Toxicol 2019;39:556-570.

39. Schoemaker MH, Conde de la Rosa L, Buist-Homan M, Vrenken TE, Havinga R, Poelstra K, Haisma HJ, et al. Tauroursodeoxycholic acid protects rat hepatocytes from bile acid-induced apoptosis via activation of survival pathways. Hepatology 2004;39:1563-1573.

40. Chan LL, McCulley KJ, Kessel SL. Assessment of Cell Viability with Single-, Dual-, and Multi-Staining Methods Using Image Cytometry. Methods Mol Biol 2017;1601:27-41.

41. Wang G, Memin E, Murali I, Gaspers LD. The effect of chronic alcohol consumption on mitochondrial calcium handling in hepatocytes. Biochem J 2016;473:3903-3921.

42. Woudenberg-Vrenken TE, Conde de la Rosa L, Buist-Homan M, Faber KN, Moshage H. Metformin protects rat hepatocytes against bile acid-induced apoptosis. PLoS One 2013;8:e71773.

43. Thery C, Amigorena S, Raposo G, Clayton A. Isolation and characterization of exosomes from cell culture supernatants and biological fluids. Curr Protoc Cell Biol 2006;Chapter 3:Unit 3 22.

44. Pizarro M, Solis N, Quintero P, Barrera F, Cabrera D, Rojas-de Santiago P, Arab JP, et al. Beneficial effects of mineralocorticoid receptor blockade in experimental non-alcoholic steatohepatitis. Liver Int 2015;35:2129-2138.

45. Suzuki E, Matsunaga T, Aonuma A, Sasaki T, Nagata K, Ohmori S. Effects of hypoxia-inducible factor-1alpha chemical stabilizer, CoCl(2) and hypoxia on gene expression of CYP3As in human fetal liver cells. Drug Metab Pharmacokinet 2012;27:398-404.

46. Wu D, Yotnda P. Induction and testing of hypoxia in cell culture. J Vis Exp 2011.

47. Sun Q, Gao W, Loughran P, Shapiro R, Fan J, Billiar TR, Scott MJ. Caspase 1 activation is protective against hepatocyte cell death by up-regulating beclin 1 protein

and mitochondrial autophagy in the setting of redox stress. J Biol Chem 2013;288:15947-15958.

48. Egnatchik RA, Leamy AK, Noguchi Y, Shiota M, Young JD. Palmitate-induced activation of mitochondrial metabolism promotes oxidative stress and apoptosis in H4IIEC3 rat hepatocytes. Metabolism 2014;63:283-295.

49. Garcia-Ruiz C, Fernandez-Checa JC. Mitochondrial Oxidative Stress and Antioxidants Balance in Fatty Liver Disease. Hepatol Commun 2018;2:1425-1439.

50. Masarone M, Rosato V, Dallio M, Gravina AG, Aglitti A, Loguercio C, Federico A, et al. Role of Oxidative Stress in Pathophysiology of Nonalcoholic Fatty Liver Disease. Oxid Med Cell Longev 2018;2018:9547613.

51. He Y, Sadahiro T, Noh SI, Wang H, Todo T, Chai NN, Klein AS, et al. Flow cytometric isolation and phenotypic characterization of two subsets of ED2(+) (CD163) hepatic macrophages in rats. Hepatol Res 2009;39:1208-1218.

52. Younossi ZM. Non-alcoholic fatty liver disease - A global public health perspective. J Hepatol 2019;70:531-544.

53. Mesarwi OA, Shin MK, Bevans-Fonti S, Schlesinger C, Shaw J, Polotsky VY. Hepatocyte Hypoxia Inducible Factor-1 Mediates the Development of Liver Fibrosis in a Mouse Model of Nonalcoholic Fatty Liver Disease. PLoS One 2016;11:e0168572.

54. Chen J, Chen J, Fu H, Li Y, Wang L, Luo S, Lu H. Hypoxia exacerbates nonalcoholic fatty liver disease via the HIF-2alpha/PPARalpha pathway. Am J Physiol Endocrinol Metab 2019;317:E710-E722.

55. Kong D, Zhang F, Shao J, Wu L, Zhang X, Chen L, Lu Y, et al. Curcumin inhibits cobalt chloride-induced epithelial-to-mesenchymal transition associated with

interference with TGF-beta/Smad signaling in hepatocytes. Lab Invest 2015;95:1234-1245.

56. Ricchi M, Odoardi MR, Carulli L, Anzivino C, Ballestri S, Pinetti A, Fantoni LI, et al. Differential effect of oleic and palmitic acid on lipid accumulation and apoptosis in cultured hepatocytes. J Gastroenterol Hepatol 2009;24:830-840.

57. Mylonis I, Simos G, Paraskeva E. Hypoxia-Inducible Factors and the Regulation of Lipid Metabolism. Cells 2019;8.

58. Mylonis I, Sembongi H, Befani C, Liakos P, Siniossoglou S, Simos G. Hypoxia causes triglyceride accumulation by HIF-1-mediated stimulation of lipin 1 expression. J Cell Sci 2012;125:3485-3493.

59. Jahn D, Kircher S, Hermanns HM, Geier A. Animal models of NAFLD from a hepatologist's point of view. Biochim Biophys Acta Mol Basis Dis 2019;1865:943-953.

60. Moravcova A, Cervinkova Z, Kucera O, Mezera V, Rychtrmoc D, Lotkova H. The effect of oleic and palmitic acid on induction of steatosis and cytotoxicity on rat hepatocytes in primary culture. Physiol Res 2015;64 Suppl 5:S627-636.

61. Wu J, Lin S, Wan B, Velani B, Zhu Y. Pyroptosis in Liver Disease: New Insights into Disease Mechanisms. Aging Dis 2019;10:1094-1108.

62. Mari M, Caballero F, Colell A, Morales A, Caballeria J, Fernandez A, Enrich C, et al. Mitochondrial free cholesterol loading sensitizes to TNF- and Fas-mediated steatohepatitis. Cell Metab 2006;4:185-198.

63. Dixon LJ, Flask CA, Papouchado BG, Feldstein AE, Nagy LE. Caspase-1 as a central regulator of high fat diet-induced non-alcoholic steatohepatitis. PLoS One 2013;8:e56100.

64. Tang Y, Cao G, Min X, Wang T, Sun S, Du X, Zhang W. Cathepsin B inhibition ameliorates the non-alcoholic steatohepatitis through suppressing caspase-1 activation. J Physiol Biochem 2018;74:503-510.

65. Panchanathan R, Liu H, Choubey D. Hypoxia primes human normal prostate epithelial cells and cancer cell lines for the NLRP3 and AIM2 inflammasome activation. Oncotarget 2016;7:28183-28194.

66. Guillot A, Tacke F. Liver Macrophages: Old Dogmas and New Insights. Hepatol Commun 2019;3:730-743.

67. Momen-Heravi F, Saha B, Kodys K, Catalano D, Satishchandran A, Szabo G. Increased number of circulating exosomes and their microRNA cargos are potential novel biomarkers in alcoholic hepatitis. J Transl Med 2015;13:261.

68. Wu X, Chang SC, Jin J, Gu W, Li S. NLRP3 in fl ammasome mediates chronic intermittent hypoxia-induced renal injury implication of the microRNA-155/FOXO3a signaling pathway. J Cell Physiol 2018;233:9404-9415.

69. Alegre F, Pelegrin P, Feldstein AE. Inflammasomes in Liver Fibrosis. Semin Liver Dis 2017;37:119-127.

70. Wei Q, Mu K, Li T, Zhang Y, Yang Z, Jia X, Zhao W, et al. Deregulation of the NLRP3 inflammasome in hepatic parenchymal cells during liver cancer progression. Lab Invest 2014;94:52-62.

**FIGURE LEGENDS**

**Figure 1. Chemical hypoxia stabilizes HIF-1α.** Primary hepatocytes were incubated for 24 h with oleic acid and palmitic acid (2:1 ratio) (FFA) in the presence or absence of CoCl2 200 µmol/L. Protein levels of HIF-1α was determined by Western Blot as described in Material and Methods. α-Tubulin was used as loading control. Data is shown as mean ± SEM (n ≥ 3) * indicates P < 0.05 and ** indicates P < 0.01.

**Figure 2. Steatosis *in vitro*: Free fatty acids and chemical hypoxia treatment increase hepatocellular content of triglycerides.** Primary hepatocytes were incubated for 24h with oleic acid and palmitic acid (2:1 ratio) (FFA) in the presence or absence of CoCl2 200 µmol/L. a) Oil Red O staining (scale bar: 40 µm) and b) Triglyceride (TG) content were measured as described in Materials and Methods. Data is shown as mean ± SEM (n ≥ 3) *** indicates P < 0.005 and **** indicates P < 0.001.

**Figure 3. Chemical hypoxia increases cleaved Caspase-3 and Caspase-3 activity in fat-laden hepatocytes.** Primary hepatocytes were incubated for 24h with oleic acid and palmitic acid (2:1 ratio) (FFA) in the presence or absence of CoCl2 200 µmol/L**.** a) Cleaved Caspase-3 protein levels and b) Caspase-3 activity were measured as described in Materials and Methods. Data is shown as mean ± SEM (n ≥ 3) * indicates P < 0.05; *** indicates P < 0.005 and **** indicates P < 0.001.

**Figure 4. Hypoxia promotes pyroptotic cell death in fat-laden hepatocytes.** Primary hepatocytes were incubated for 24h with free fatty acids (FFA) [oleic acid and palmitic acid (2:1 ratio)] in the presence or absence of CoCl2 200 µmol/L**.** a) SYTOX™ green [Representative images (upper panel)] and quantification (lower panel), b) LDH leakage into culture medium and c) GSDMD-N protein levels determined by Western

Blot as described in Materials and Methods. Data were shown as mean ± SEM (n ≥ 3) * indicates P < 0.05 and ** indicates P < 0.01.

**Figure 5. Hypoxia increases mitochondrial superoxide levels in steatotic hepatocytes**. Primary hepatocytes were incubated for 24h with oleic acid and palmitic acid (2:1 ratio) (FFA) in the presence or absence of CoCl2 200 µmol/L. Superoxide generation by mitochondria was determined using MitoSOX™ fluorogenic probe as described in Materials and Methods. Data is shown as mean ± SEM (n ≥ 3) ** indicates P < 0.01 and *** indicates P < 0.005.

**Figure 6. Hypoxia increases the expression of pro-inflammatory cytokines in steatotic hepatocytes.** Primary hepatocytes were incubated for 24h with oleic acid and palmitic acid (2:1 ratio) (FFA) in the presence or absence of CoCl2 200 µmol/L. mRNA levels of interleukin (IL)-1β, tumor necrosis factor (TNF)-α and IL-6 were measured as described in Materials and Methods. Data is shown as mean ± SEM (n ≥ 3) * indicates P < 0.05; ** indicates P < 0.01; *** indicates P < 0.005 and **** indicates P < 0.001.

**Figure 7. Hypoxia increases cleaved caspase-1 protein levels in steatotic hepatocytes**. Primary hepatocytes were incubated for 24h with oleic acid and palmitic acid (2:1 ratio) (FFA) in the presence or absence of CoCl2 200 µmol/L. Protein levels of pro-caspase-1 and cleaved caspase-1 (p10 and p20) were determined by Western Blot as described in Materials and Methods. α-Tubulin was used as loading control. The sum of p20 and p10 caspase-1 was calculated to determine the generation of cleaved Caspase-1. Data is shown as mean ± SEM (n ≥ 3) * indicates P < 0.05; ** indicates P < 0.01 and *** indicates P < 0.005.

**Figure 8. Characterization of Kupffer cells by immunofluorescence.** Purity of isolated Kupffer cell (KCs) was assessed by cell staining with specific Kupffer cell green fluorescent marker CD163 (a) and macrophage red fluorescent marker CD68 (b). Nuclei were stained blue with DAPI as described in Materials and Methods (Supplementary materials). Scale bar: 10 μm

**Figure 9. Conditioned medium of steatotic hepatocytes subjected to hypoxia increases gene expression of pro-inflammatory genes and IL-1β protein levels in Kupffer cells (KC).** Primary hepatocytes were incubated for 24h with oleic acid and palmitic acid (2:1 ratio) (FFA) in the presence or absence of CoCl2 200 μmol/L. Then, culture medium of primary hepatocytes was replaced with free fatty acids FFA and CoCl2-free medium for an additional 24 hours to obtain conditioned medium (CM). KC were treated for 24 hours with the CM from cultured hepatocytes from different experimental groups. a) mRNA levels of interleukin (IL)-1β, tumor necrosis factor (TNF)-α, inducible nitric oxide synthase (iNOS), IL-6, IL-10 and Arginase (Arg-1) and b) IL-1β protein levels were assessed by ELISA as described in Materials and Methods. Data is shown as mean ± SEM ($n \geq 3$) * indicates $P < 0.05$; ** indicates $P < 0.01$; *** indicates $P < 0.005$; **** indicates $P < 0.001$.

**Figure 10. EVs obtained from culture media of fat-laden HepG2 cells exposed to CoCl2 increases pro-inflammatory genes in Kupffer Cells (KC).** Presence of EVs was confirmed by electron microscopy (a) transmission and quantified using Nano tracking analysis (b). Free fatty acids (FFA) and CoCl2 treatment of HepG2 cells determined an increase in the number of EVs in cultured media with no significant changes in their size. KC were treated with hypoxic and fat-laden HepG2 cells-derived

EVs (15 μg) and EV-free culture media as negative control. mRNA levels of interleukin (IL)-1β, tumor necrosis factor TNF-α, inducible nitric oxide synthase (iNOS), IL-6, IL-10 and Arginase -1 (Arg-1) were measured as described in Materials and Methods. Data is shown as mean ± SEM (n ≥ 3) * indicates P < 0.05; ** indicates P < 0.01; *** indicates P < 0.005; **** indicates P < 0.001.

**Figure 11. Intermittent hypoxia increased histological steatosis in mice with CDAA-induced liver injury determined by Oil Red-O staining, without changes in hepatic triglyceride**. Mice were placed on choline-supplemented L-amino acid defined (CSAA) diet as control, or defined diet with choline deficiency amino acids (CDAA) for 22 weeks to induce liver injury and intermittent hypoxia (IH) or normoxia was applied for the last 12 weeks of the diet as described in Materials and Methods. a) Liver sections were stained with Oil Red O and analyzed by a pathologist in a blinded fashion to determine b) steatosis score as described in Materials and Methods. c) Hepatic triglyceride content was measured as described in Materials and Methods. Data were shown as mean ± SEM (n ≥ 3) ** indicates P < 0.01; *** indicates P < 0.005 and **** indicates P < 0.001.

**Figure 12. Intermittent hypoxia in mice with CDAA-induced liver injury increases the expression of pro-inflammatory cytokines and inflammasome components**. Mice were placed on choline-supplemented L-amino acid defined (CSAA) diet as control, or defined diet with choline deficiency amino acids (CDAA) for 22 weeks to induce liver injury and intermittent hypoxia (IH) or normoxia was applied for the last 12 weeks of the diet as described in Materials and Methods. mRNA levels of interleukin (IL)-1β, IL-18, NLRP3, caspase-1, IL-6 and interferon (IFN)-γ

were measured as described in Materials and Methods. Data is shown as mean ± SEM (n ≥ 3) * indicates P < 0.05; ** indicates P < 0.01; *** indicates P < 0.005; **** indicates P < 0.001.

**Figura 13. Intermittent hypoxia in mice with CDAA-induced liver injury increases cleaved caspase-1**. Mice were placed on choline-supplemented L-amino acid defined (CSAA) diet as control, or defined diet with choline deficiency amino acids (CDAA) for 22 weeks to induce liver injury and intermittent hypoxia (IH) or normoxia was applied for the last 12 weeks of the diet as described in Materials and Methods. Protein levels of pro-caspase-1 and cleaved caspase-1 (p10 and p20) were determined by Western Blot as described in Materials and Methods. α-Tubulin was used as a loading control. The sum of p20 and p10 caspase-1 was calculated to determine the generation of cleaved caspase-1. Data were shown as mean ± SEM (n ≥ 3) ** indicates P < 0.01 and *** indicates P < 0.005.

**Declaration of interests**

☒ The authors declare that they have no known competing financial interests or personal relationships that could have appeared to influence the work reported in this paper.

☐The authors declare the following financial interests/personal relationships which may be considered as potential competing interests:

## Highlights

- Obstructive sleep apnea syndrome (OSAS) is an aggravating factor of non-alcoholic fatty liver disease (NAFLD).
- The effects of cobalt chloride-induced chemical hypoxia on fat-laden hepatocytes were explored
- Hypoxia amplified hepatocellular damage, promote inflammation and determine increased expression of inflammasome components.
- Intermittent hypoxia in mice with steatohepatits also promoted a pro-inflammatory phenotype and inflammasome activation
- Evidence of a crosstalk between steatotic hepatocytes undergoing hypoxia and Kupffer cells mediated in part by extracellular vesicles was found.

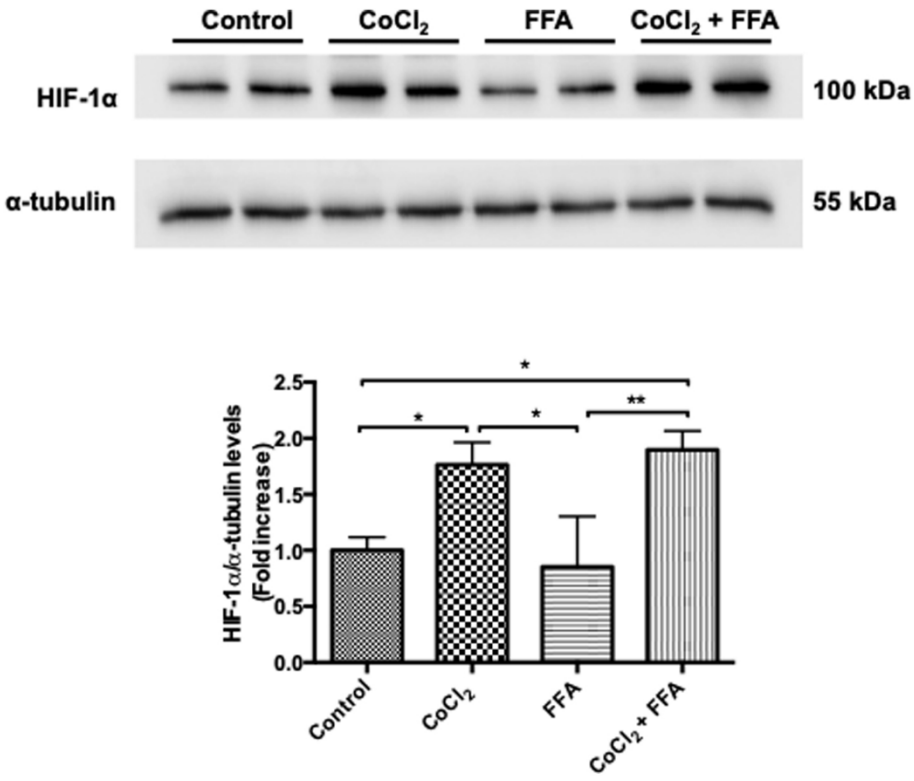
Control
CoCl2
FFA
CoCl2 + FFA
HIF-1α
100 kDa
α-tubulin
55 kDa
HIF-1αα-tubulin levels
(Fold increase)
2.5
2.0
1.5
1.0
0.5
0.0
*
*
*
**
Control
CoCl2
FFA
CoCl2 + FFA

Figure 1

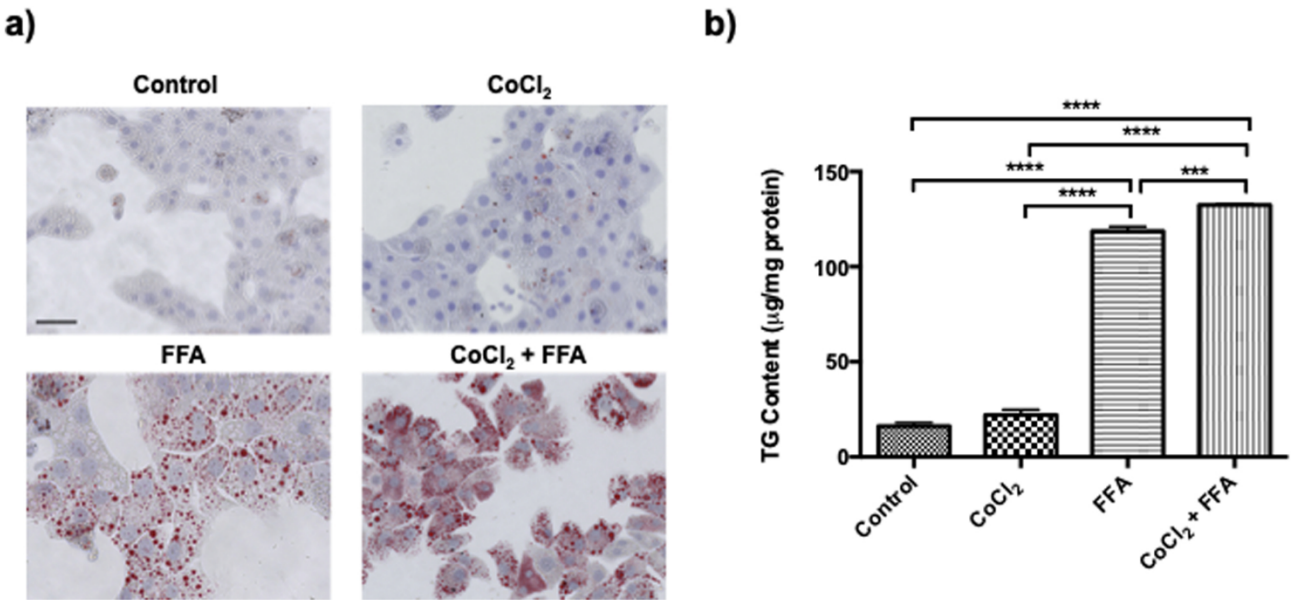
a)
Control
CoCl2
FFA
CoCl2 + FFA
b)
TG Content (μg/mg protein)
150
100
50
0
****
****
****
****
***
Control
CoCl2
FFA
CoCl2 + FFA

Figure 2

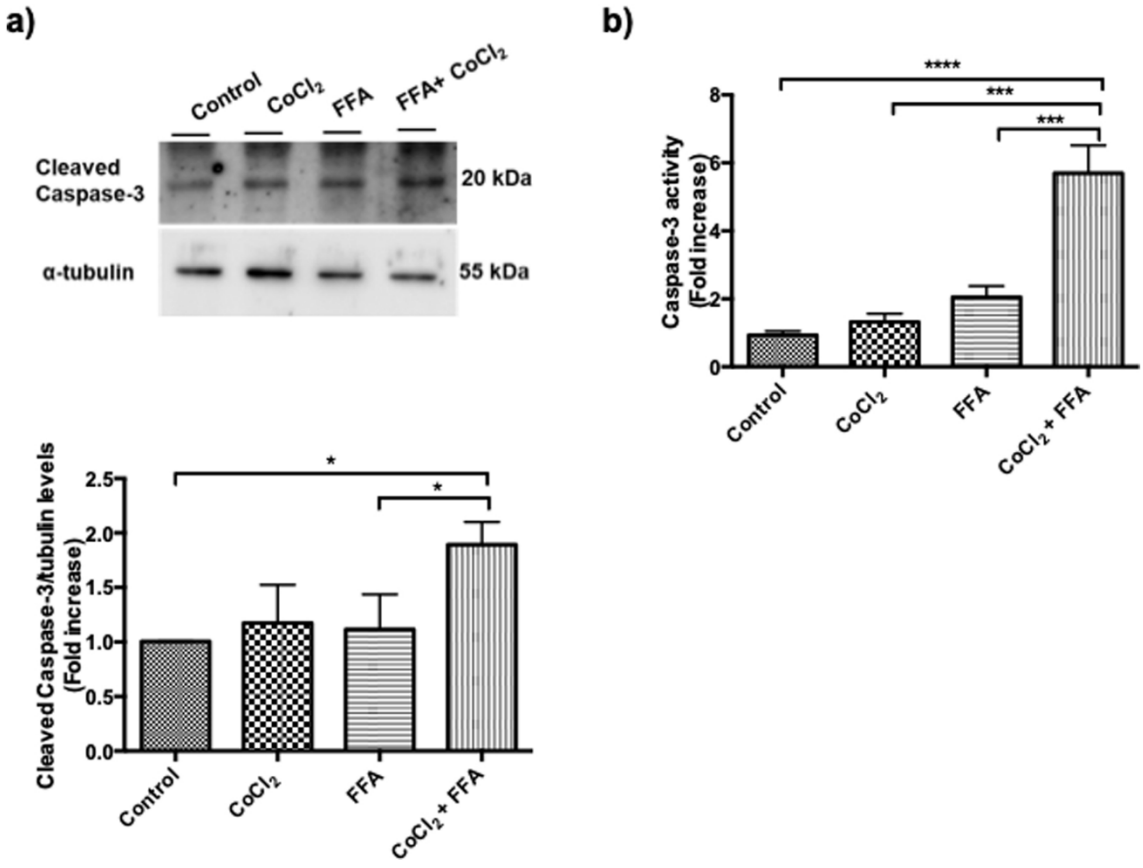
a)
Control
CoCl2
FFA
FFA+ CoCl2
Cleaved Caspase-3
20 kDa
α-tubulin
55 kDa
Cleaved Caspase-3/tubulin levels (Fold increase)
2.5
2.0
1.5
1.0
0.5
0.0
*
*
Control
CoCl2
FFA
CoCl2 + FFA
b)
Caspase-3 activity (Fold increase)
8
6
4
2
0
****
***
***
Control
CoCl2
FFA
CoCl2 + FFA

Figure 3

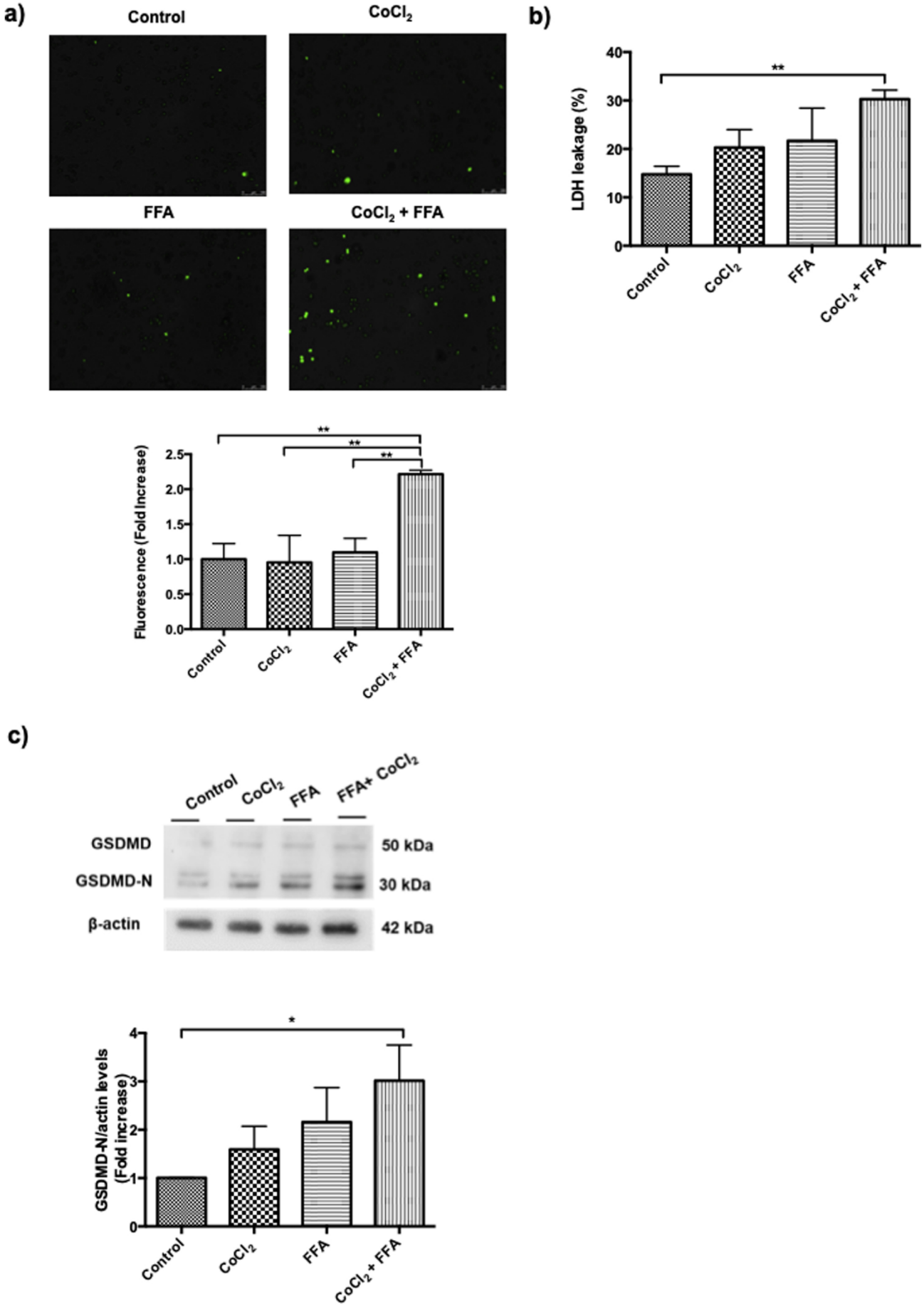
a)
Control
CoCl2
FFA
CoCl2 + FFA
Fluorescence (Fold Increase)
2.5
2.0
1.5
1.0
0.5
0.0
**
**
**
Control
CoCl2
FFA
CoCl2 + FFA
b)
LDH leakage (%)
40
30
20
10
0
**
Control
CoCl2
FFA
CoCl2 + FFA
c)
Control
CoCl2
FFA
FFA+ CoCl2
GSDMD
GSDMD-N
β-actin
50 kDa
30 kDa
42 kDa
GSDMD-N/actin levels (Fold increase)
4
3
2
1
0
*
Control
CoCl2
FFA
CoCl2 + FFA

Figure 4

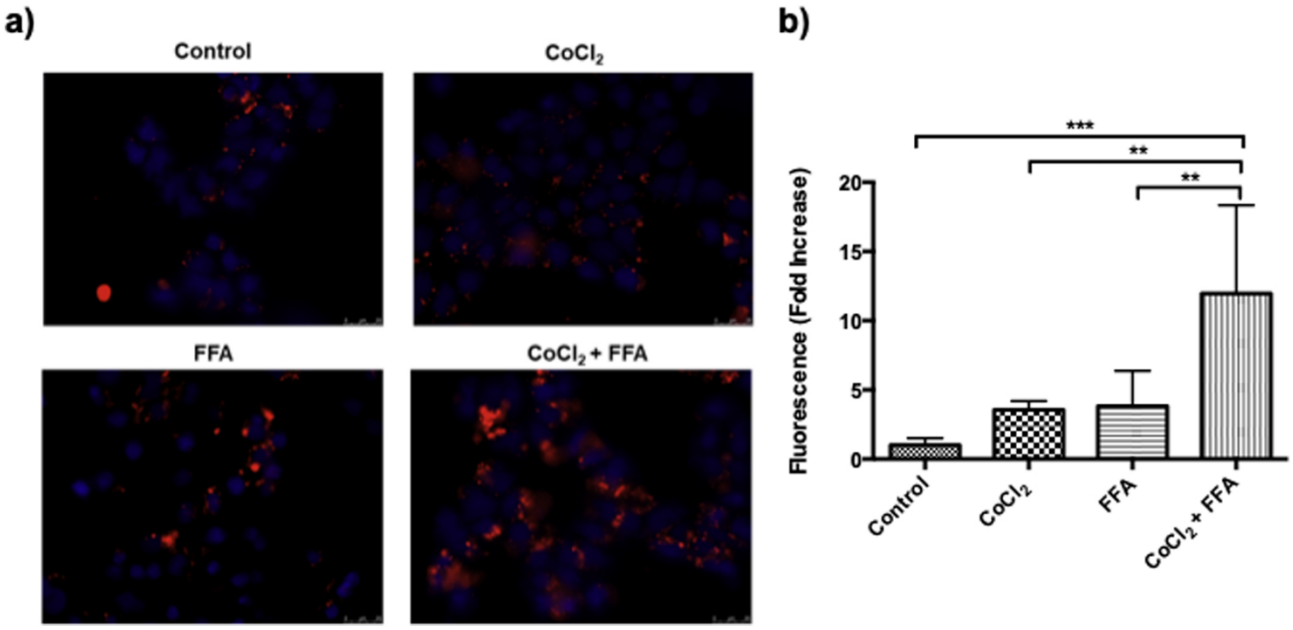
a)
Control
CoCl2
FFA
CoCl2 + FFA
b)
Fluorescence (Fold Increase)
20
15
10
5
0
***
**
**
Control
CoCl2
FFA
CoCl2 + FFA

Figure 5

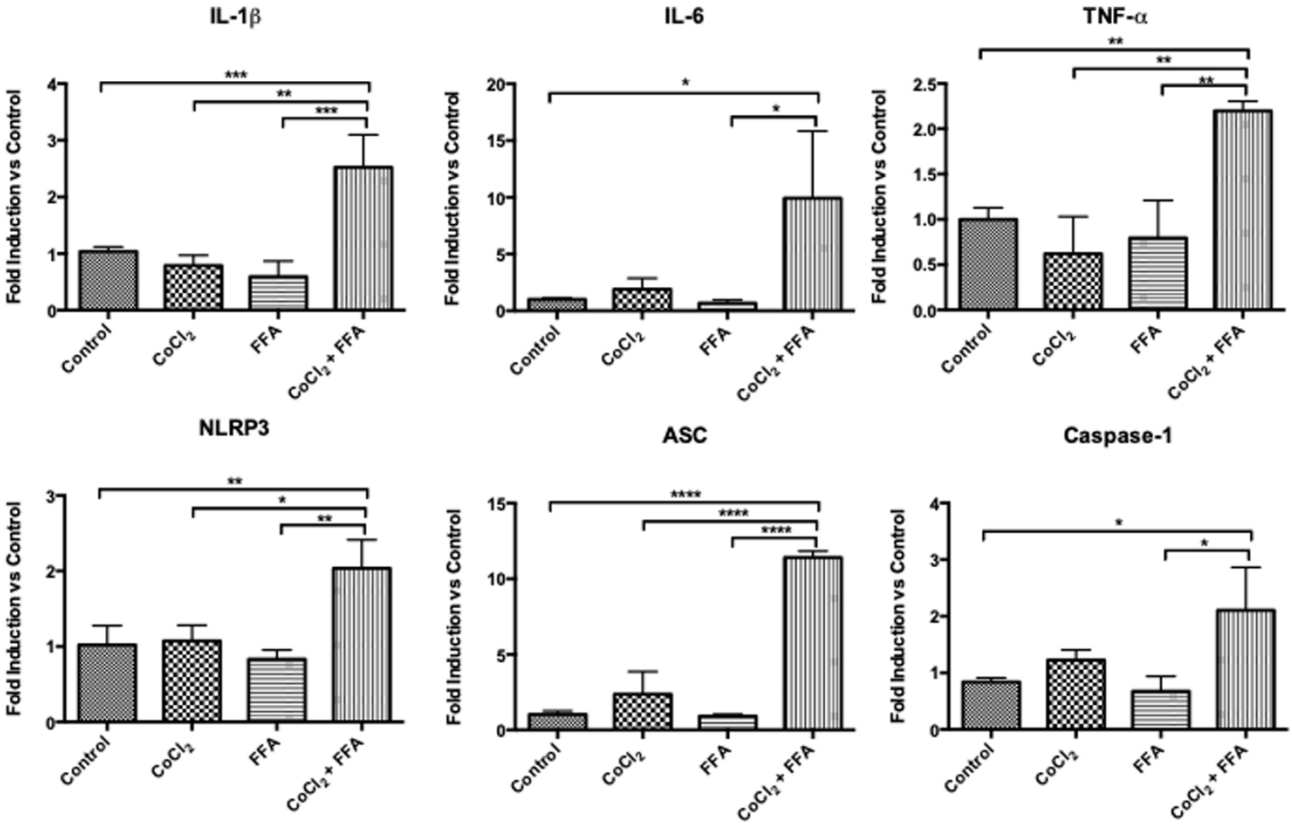
IL-1β
IL-6
TNF-α
NLRP3
ASC
Caspase-1
Fold Induction vs Control
Control
CoCl2
FFA
CoCl2 + FFA

Figure 6

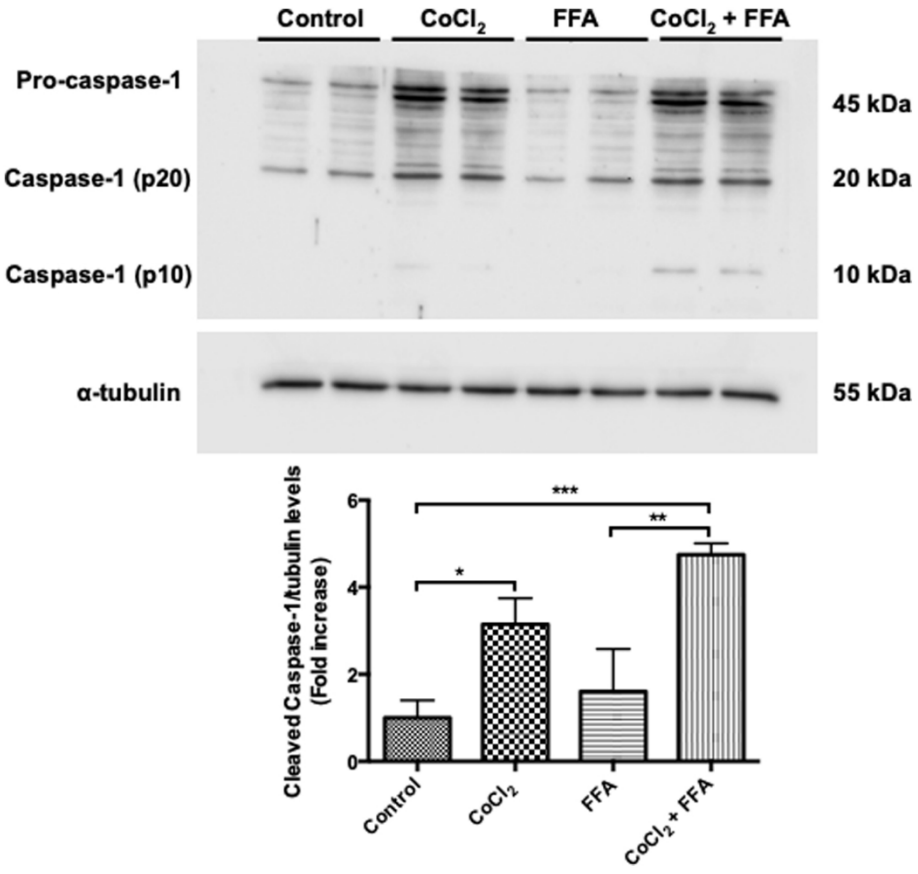
Control
CoCl2
FFA
CoCl2 + FFA
Pro-caspase-1
Caspase-1 (p20)
Caspase-1 (p10)
45 kDa
20 kDa
10 kDa
α-tubulin
55 kDa
Cleaved Caspase-1/tubulin levels
(Fold increase)
6
4
2
0
*
**
***
Control
CoCl2
FFA
CoCl2 + FFA

Figure 7

a)

b)

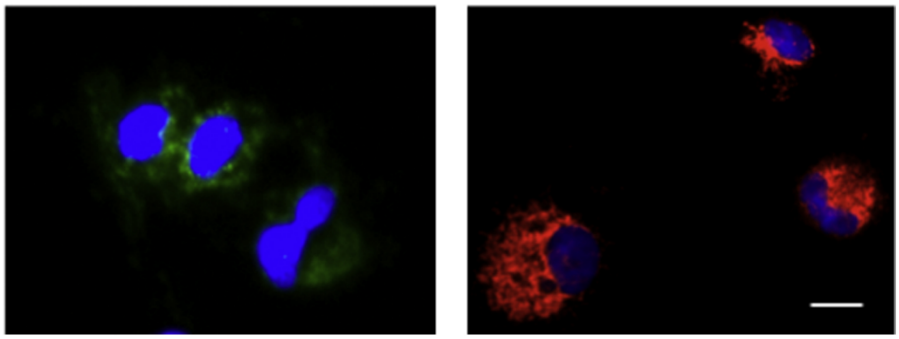

Figure 8

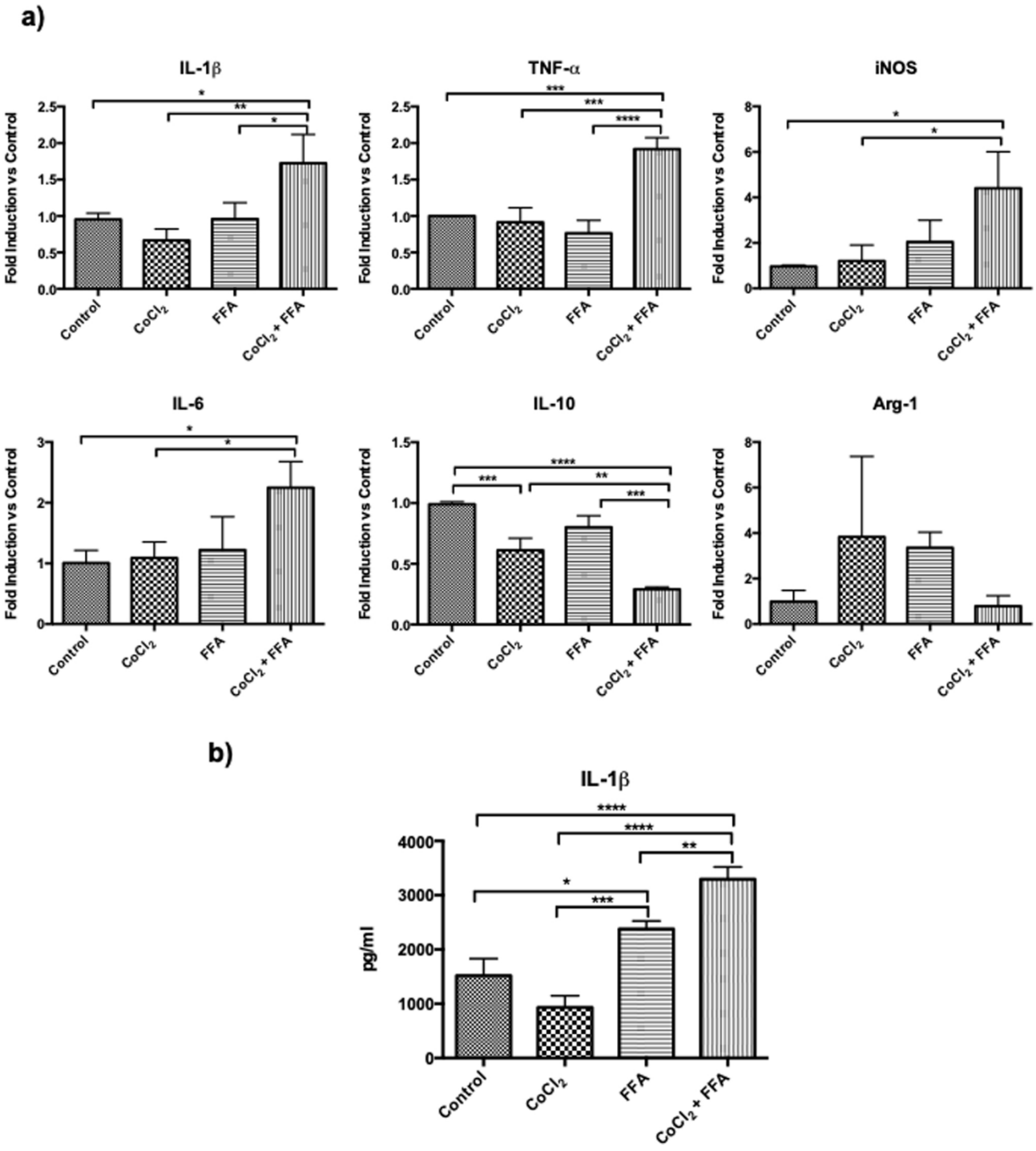
a)
IL-1β
TNF-α
iNOS
IL-6
IL-10
Arg-1
Fold Induction vs Control
Control
CoCl2
FFA
CoCl2 + FFA
b)
IL-1β
pg/ml
Control
CoCl2
FFA
CoCl2 + FFA

Figure 9

a)

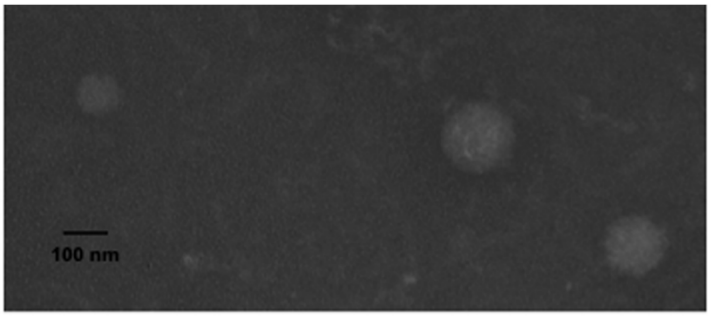
100 nm

b)

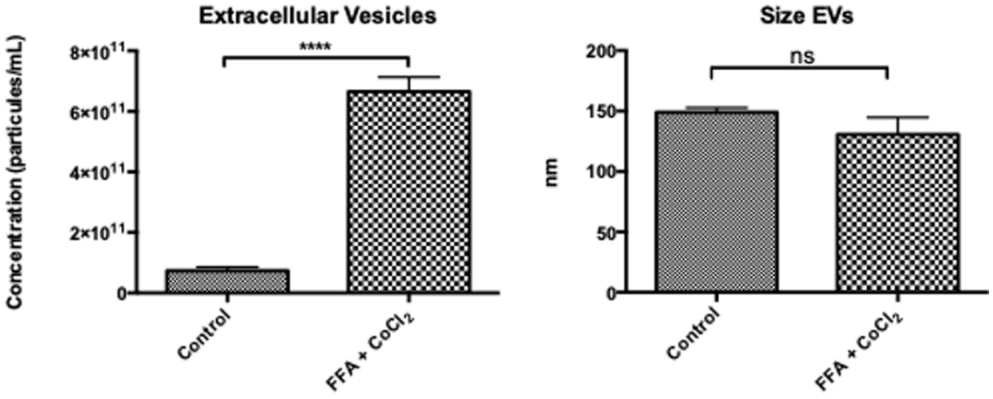
Extracellular Vesicles
Concentration (particules/mL)
8×10^11
6×10^11
4×10^11
2×10^11
0
****
Control
FFA + CoCl2
Size EVs
nm
200
150
100
50
0
ns
Control
FFA + CoCl2

Figure 10

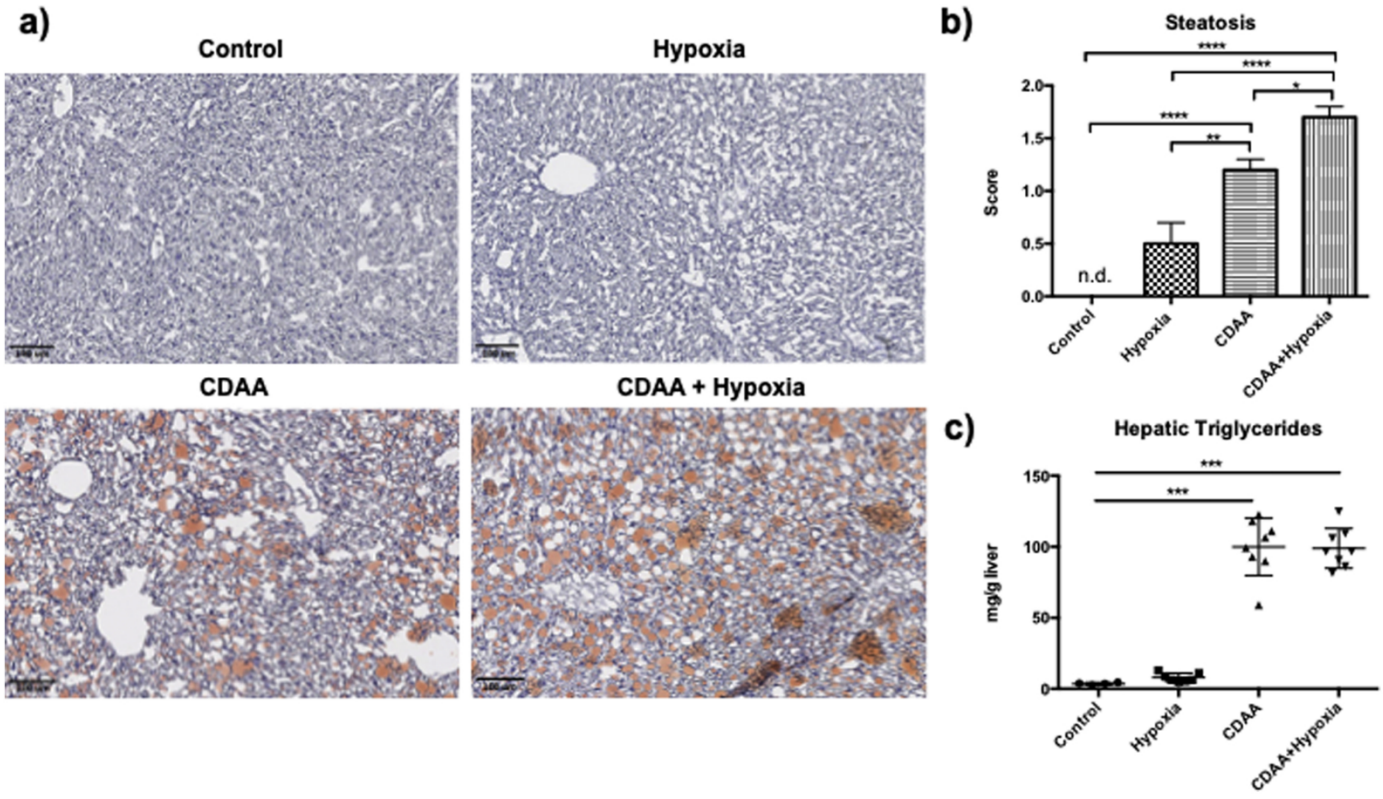
a)
Control
Hypoxia
CDAA
CDAA + Hypoxia
b)
Steatosis
Score
n.d.
Control
Hypoxia
CDAA
CDAA+Hypoxia
c)
Hepatic Triglycerides
mg/g liver
Control
Hypoxia
CDAA
CDAA+Hypoxia

Figure 11

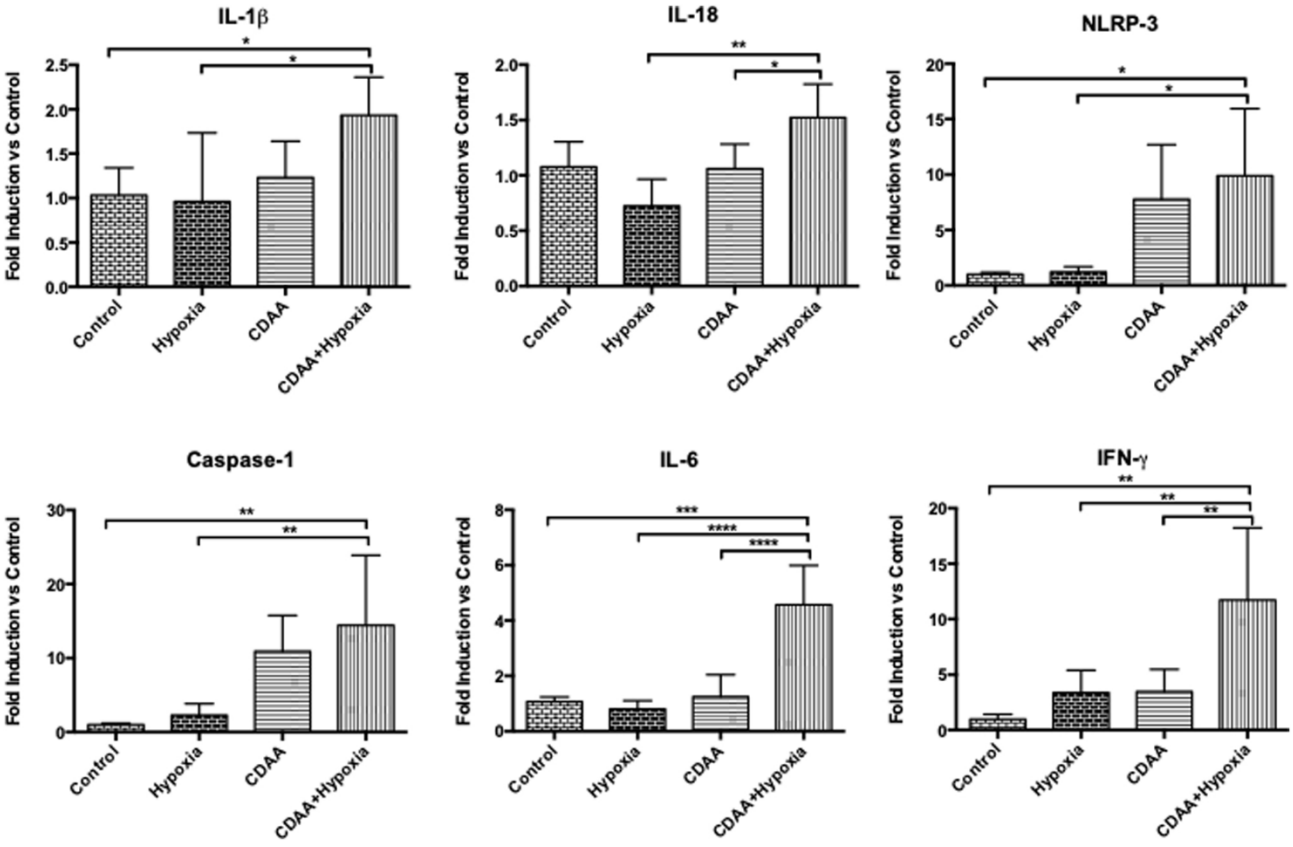
IL-1β
IL-18
NLRP-3
Caspase-1
IL-6
IFN-γ
Fold Induction vs Control
Control
Hypoxia
CDAA
CDAA+Hypoxia

Figure 12

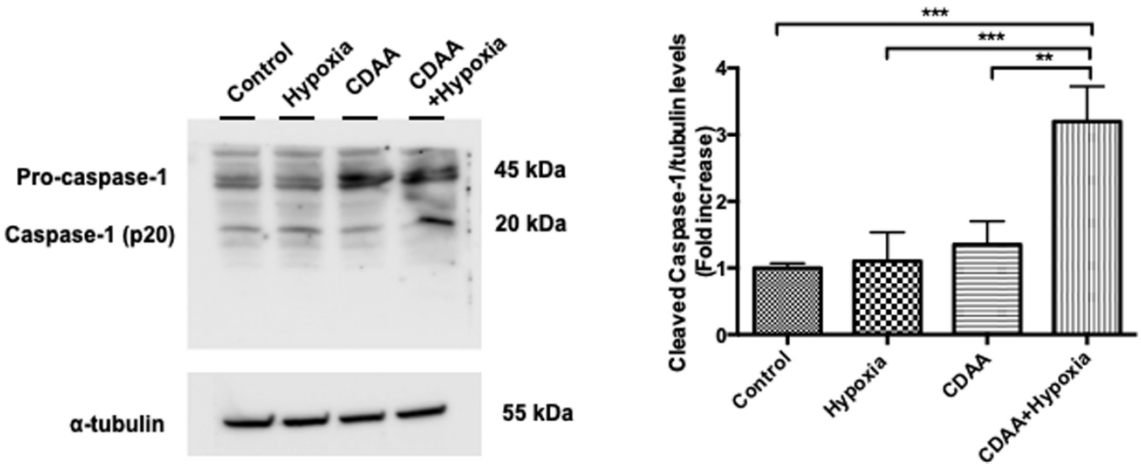
Control
Hypoxia
CDAA
CDAA +Hypoxia
Pro-caspase-1
Caspase-1 (p20)
45 kDa
20 kDa
α-tubulin
55 kDa
***
***
**
Cleaved Caspase-1/tubulin levels (Fold increase)
0
1
2
3
4
Control
Hypoxia
CDAA
CDAA+Hypoxia

Figure 13

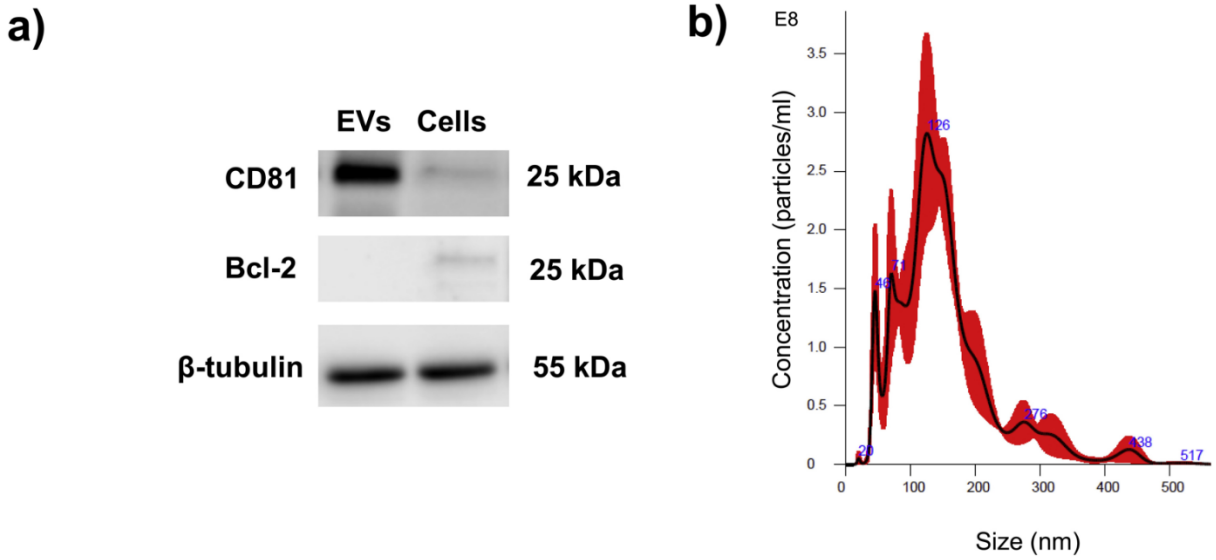
a)
EVs
Cells
CD81
25 kDa
Bcl-2
25 kDa
β-tubulin
55 kDa
b)
E8
Concentration (particles/ml)
Size (nm)
126
71
46
278
438
517
29

Figure 14

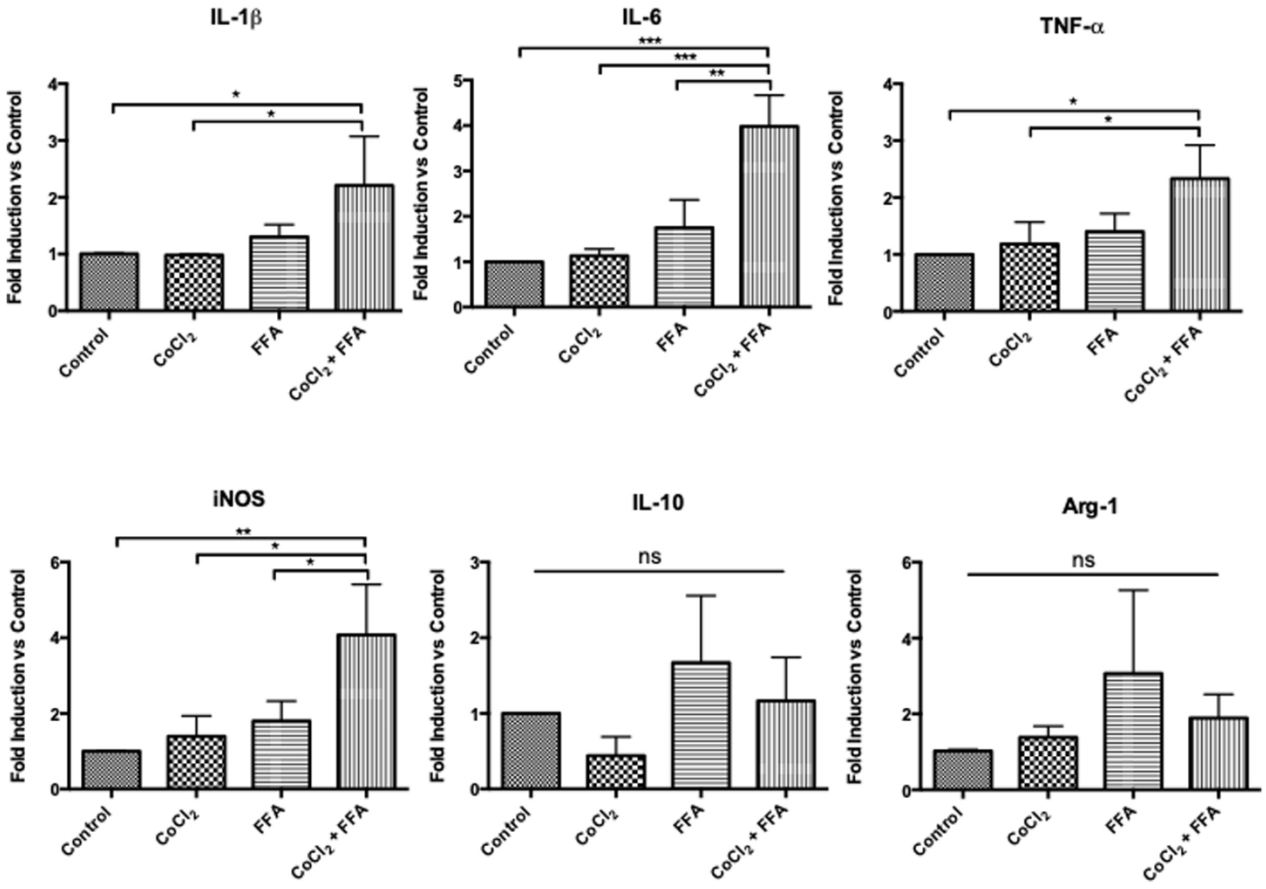
IL-1β
Fold Induction vs Control
Control
CoCl2
FFA
CoCl2 + FFA
IL-6
TNF-α
iNOS
IL-10
ns
Arg-1

Figure 15

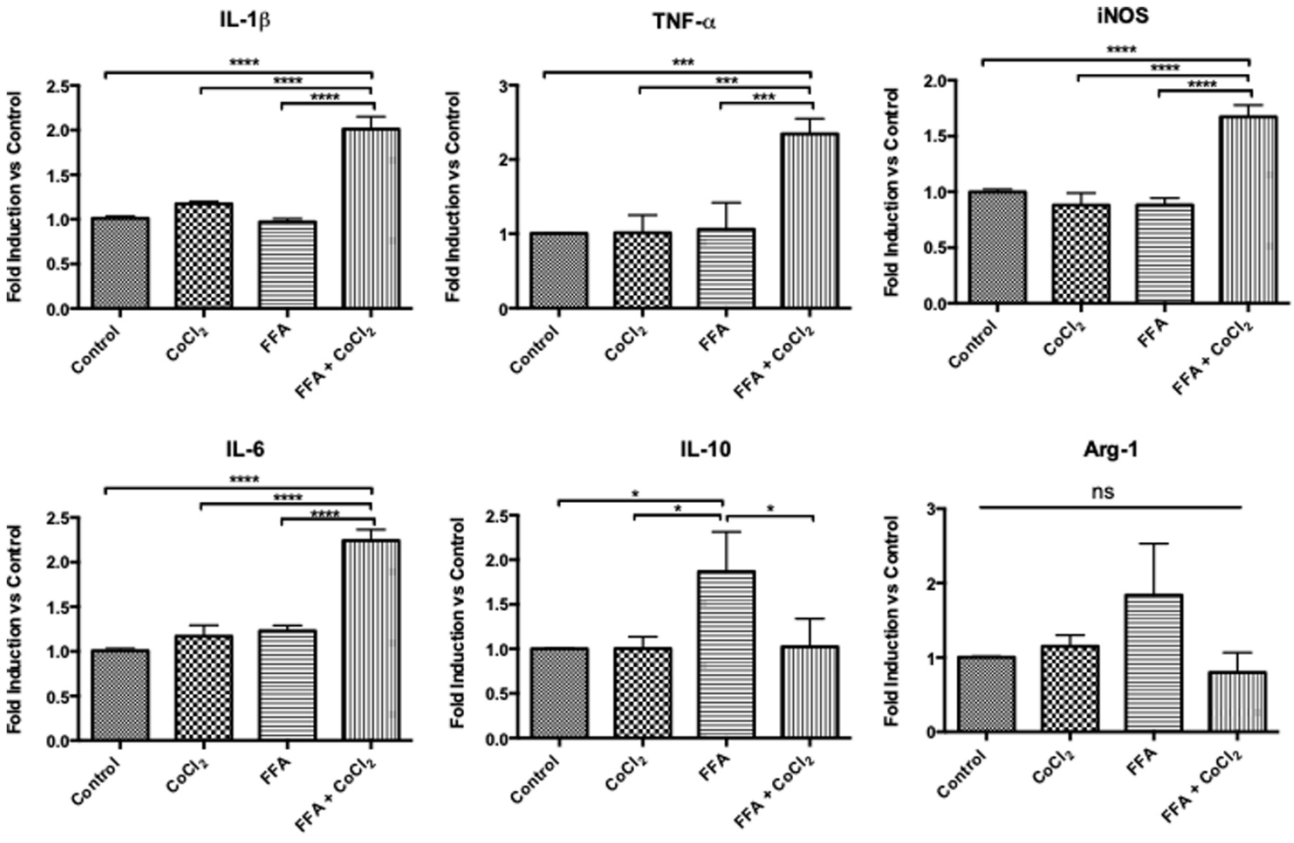
IL-1β
TNF-α
iNOS
IL-6
IL-10
Arg-1
Fold Induction vs Control
Control
CoCl2
FFA
FFA + CoCl2
****
***
*
ns

Figure 16

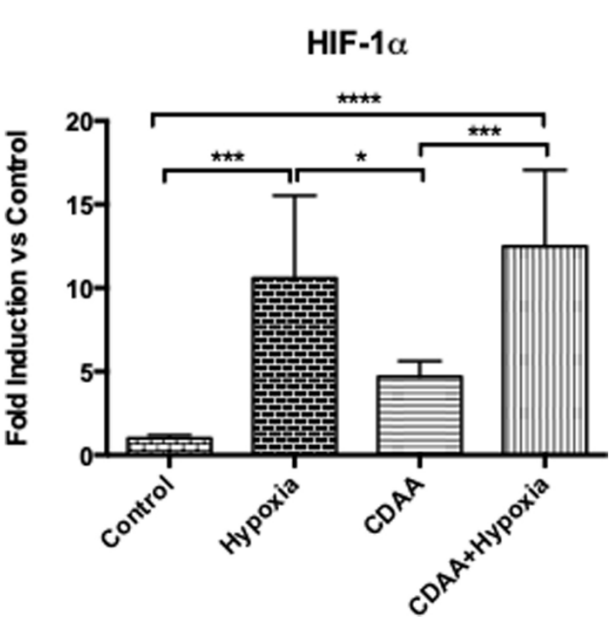
HIF-1α
Fold Induction vs Control
20
15
10
5
0
****
***
*
***
Control
Hypoxia
CDAA
CDAA+Hypoxia

Figure 17